Univerzita Karlova v Praze
Matematicko-fyzikální fakulta

**DIPLOMOVÁ PRÁCE**

Jaroslav Hamerský

# Magnetické pole v jádru Galaxie

Astronomický ústav UK

Vedoucí diplomové práce: Doc.RNDr.Vladimír Karas,DrSc.
Studijní program: Fyzika
Studijní obor: Astronomie a astrofyzika

Praha 2011

Na tomto místě bych rád poděkoval vedoucímu své diplomové práce Doc.RNDr.Vladimíru Karasovi,DrSc. za čas, který mi věnoval a za důležité rady a podněty bez nichž by nebylo možné tuto práci sepsat. Také bych chtěl poděkovat Grantové agentuře Univerzity Karlovy, jejíž finanční prostředky mi umožnily naplno se věnovat danému tématu.

Prohlašuji, že jsem tuto diplomovou práci vypracoval(a) samostatně a výhradně s použitím citovaných pramenů, literatury a dalších odborných zdrojů.

Beru na vědomí, že se na moji práci vztahují práva a povinnosti vyplývající ze zákona č. 121/2000 Sb., autorského zákona v platném znění, zejména skutečnost, že Univerzita Karlova v Praze má právo na uzavření licenční smlouvy o užití této práce jako školního díla podle §60 odst. 1 autorského zákona.

V ..... dne ..... Podpis autora

Název práce: Magnetické pole v jádru Galaxie

Autor: Jaroslav Hamerský

Katedra: Astronomický ústav UK

Vedoucí diplomové práce: Doc.RNDr.Vladimír Karas,DrSc., Astronomický ústav AV ČR, v.v.i.

Abstrakt: V předložené práci studujeme chování akrečních disků v blízkosti Černé díry. Náš přístup k této problematice vychází z řešení obecně relativistických magnetohydrodynamických rovnic, které plynou ze zákonů zachování tenzoru energie a hybnosti a počtu částic a Maxwellových rovnic. Tyto rovnice řešíme numerickými metodami, jejichž shrnutí je uvedeno v první kapitole. Základní formalismus námi uvažovaných disků je zpracován ve druhé kapitole této práce. Zajímáme se zejména o disky s konstantní hustotou momentu hybnosti a o tzv. Fisboneovy-Moncriefovy disky. U těchto disků studujeme závislost rychlosti akrece v případě náhlého zvětšení hmotnosti Černé díry a tedy narušení rovnováhy. V případě disků s konstantní hustotou momentu hybnosti nás zajímá také vliv velikosti toroidálního magnetického pole na rychlost akrece.

Klíčová slova: Obecně relativistická magnetohydrodynamika, akreční disk, černá díra

Title: Magnetic field in the Galactic centre

Author: Jaroslav Hamerský

Department: Astronomical Institute of Charles University

Supervisor: Doc.RNDr.Vladimír Karas,DrSc., Astronomical Institute of Academy of Science of Czech Republic

Abstract: In the present work we study the properties of accretion tori orbiting black hole. Our approach to this problem comes from the solving of general relativistic magnetohydrodynamic equations, which follow from conservation of the energy-momentum tensor, the particle number and from Maxwell's equations. We solve these equations by numerical methods which are described in Chapter 1. The formalism of tori which we consider here is described in Chapter 2. We are interested in tori with constant density of angular momentum and Fishbone-Moncrief tori mainly. We study accretion rates in these tori when the mass of black hole is increased suddenly and so the equilibrium in the torus is corrupted. For tori with constant density of angular momentum we study the influence of the presence of toroidal magnetic field on accretion rates.

Keywords: General relativistic MHD, accretion torus, black hole

# Contents

**Introduction** **2**

**1 General Relativistic MHD** **3**
1.1 Theoretical scheme . . . . . 3
1.2 Numerical scheme . . . . . 9

**2 Fluid tori orbiting Kerr black hole** **14**
2.1 Fishbone-Moncrief model of accretion torus: $l_*$=*const.* . . . . . 14
2.2 Abramowicz et al.model of accretion torus: $l$=*const.* . . . . . 19
2.3 Magnetized torus with the toroidal magnetic field . . . . . 23

**3 Results: axi-symmetric accretion of magnetized tori** **25**
3.1 The dependence of accretion rates on magnetic field . . . . . 25
3.2 Comparison of $l$=*const.* and $l_*$=*const.* tori . . . . . 34

**Conclusion** **38**

**Bibliography** **39**

**Appendix** **40**

# Introduction

It is commonly thought that many astrophysical systems contain relativistic plasma with a dynamically significant magnetic field. Examples include accreting black holes in black hole binaries, galactic nuclei, gamma-ray bursts, the cores of massive stars undergoing core collapse, isolated neutron stars, and neutron stars in binary systems. The kinematical gas analysis with HST (The Hubble Space Telescope) makes a convincing argument that the masses of central black holes in galaxies ranges from $10^5 M_\odot$ to more than $10^9 M_\odot$ (Kormendy & Richstone 1995). Astrophysical black holes do not support their own magnetic field, however they are embedded in cosmic magnetic field of external origin, with which they interact (Begelman et al. 1984). So we expect that the interaction of magnetized plasma with the gravitational fields of black holes permeate the Universe and the astrophysical consequences should be significant. From the observations of $SgrA^*$ it seems that the magnetic field strength can reach the value around $40G$ (Eckart et al. 2008).

Fluid mechanics is well described by hydrodynamics but including magnetic fields into the flow of fluids, gases and plasmas creates forces unknown to hydrodynamics. Thus, we have much more complicated problem which requires a new subject, magnetohydrodynamics (MHD). Even more complicated situation occurs when we combine both magnetic and gravitational interactions with plasma flows. The subject which studies such problems is called GRMHD (General Relativistic Magnetohydrodynamics) (Punsly 2008).

It is not surprising that there is an interest in numerical methods for solving the equations of GRMHD. In this work we use program HARM developed by Gammie et al. (2003) that solves hyperbolic partial differential equations in conservative form. HARM has been configured to solve the relativistic magnetohydrodynamic equations of motion on a stationary black hole spacetime in Kerr-Schild coordinates to evolve an accretion torus model.

The thesis is arranged as follows. In Chapter 1 we describe the formalism and we summarize the relevant equations as originally derived by Gammie et al. (2003). These relations are needed in order to understand the numerical approach to the solution. To this end we closely follow Gammie et al. (2003) and Noble et al. (2006). In Chapter 2 we describe three different models of accretion torus: the Fishbone-Moncrief torus, the torus with constant density of angular momentum $l = const.$ and $l = const.$ torus with the presence of toroidal magnetic field. In this chapter we follow Fishbone & Moncrief (1976), Abramowicz & Jaroszynski (1977) and Komissarov (2006). In Chapter 3 we apply the code to study axially symmetric fluid tori of Fishbone & Moncrief and Abramowicz et al. We first implement the appropriate boundary conditions and reproduce the non-magnetized stationary solutions, including the critical configurations with the relativistic cusp. Then we go over to study the case of toroidal magnetic field permeating the stationary torus.

# 1. General Relativistic MHD

## 1.1 Theoretical scheme

The conservative scheme means that the differential equations which need to be integrated are of the following form:

$$\partial_t U(P) + \partial_i F^i(P) = S(P). \tag{1.1}$$

$U$ represents the vector of "conserved" variables, such as particle number density, energy or momentum density, $F^i$ represents a vector of fluxes and $S$ is a vector of source terms that does not involve derivatives of $P$ and therefore does not affect the characteristic structure of the system. In the case when $S = 0$, the meaning of conserved variables is obvious because the rate of change of the integral of $U$ over the volume depends only on fluxes at the boundaries, by the divergence theorem. $P$ is the vector of "primitive" variables as rest-mass density, internal energy density, components of velocity and magnetic field. The fluxes and conserved variables depend on $P$. Conservative numerical schemes advance $U$ and then calculate $P(U)$ once or twice per time step depending on the order of the scheme.

In nonrelativistic conservative MHD schemes the conserved quantities are trivially related to the primitive variables. The forward transformation $P \to U$ and also the inverse transformation $U \to P$ have a closed-form solution. However, in GRMHD the $U(P)$ is a complicated nonlinear relation and the inverse transformation has no closed-form solution. So it must be treated numerically.

Throughout the whole text we adopt the geometrized units $c = G = 1$ and assume metric of the signature $-, +, +, +$. We will also use the following numbering of coordinates: $(t, r, \vartheta, \varphi) \to (0, 1, 2, 3)$.

The normal observer's ( Zero Angular Momentum Observer) four-velocity is

$$n_\mu = (-\alpha, 0, 0, 0) \tag{1.2}$$

in coordinates $t, x_1, x_2, x_3$. For the lapse function $\alpha$ one can write

$$\alpha^2 = -\frac{1}{g^{tt}}. \tag{1.3}$$

It is not trivial to see that $\alpha$ in equation (1.2) has the meaning of the lapse function since lapse function is usually defined as

$$\alpha^2 \equiv -g_{t\varphi}\omega - g_{tt}, \tag{1.4}$$

where

$$\omega \equiv -\frac{g_{t\varphi}}{g_{\varphi\varphi}}. \tag{1.5}$$

Now we prove equation (1.3), especially that the $\alpha$ in this equation is the lapse function according to definition (1.4). For the normal observer we can write the contravariant indices of his four-velocity as follows

$$n^\mu = (n^t, 0, 0, n^\varphi), \tag{1.6}$$

where $n^\varphi = n^t\omega$. Now we can use the normalization condition for four-velocities

$$g_{\mu\nu}n^\mu n^\nu = -1, \tag{1.7}$$

from which it follows that

$$n^t = \sqrt{-\frac{1}{g_{tt} + g_{t\varphi}\omega}}. \tag{1.8}$$

For covariant indices one can write

$$n_t = g_{t\mu}n^\mu = g_{tt}n^t + g_{t\varphi}n^t\omega \tag{1.9}$$

and

$$n_\varphi = g_{t\varphi}n^t + g_{\varphi\varphi}n^t\omega. \tag{1.10}$$

Thanks to the definition of lapse (1.4) we can rewrite equation (1.9) into

$$n_t = -\alpha^2 n^t. \tag{1.11}$$

If we also realize that $n^t = n_t g^{tt}$ we get

$$\alpha = \sqrt{-\frac{n_t}{n^t}} = \sqrt{-\frac{1}{g^{tt}}}. \tag{1.12}$$

So we have just showed that $\alpha^2 = -\frac{1}{g^{tt}}$ and that the expression (1.3) is consistent with our definition of the lapse function (1.4).

The fluid is described by its four-velocity $u^\mu$, the rest mass density $\rho_0$, the internal energy per unit proper volume $u$ and the pressure $p$. The electromagnetic field is described by the antisymmetric field tensor $F^{\mu\nu}$ and its dual which is defined by

$${}^*F^{\mu\nu} \equiv \frac{1}{2}\epsilon^{\mu\nu\kappa\lambda}F_{\kappa\lambda}, \tag{1.13}$$

where $\epsilon^{\mu\nu\kappa\lambda} \equiv -\frac{1}{\sqrt{-g}}[\mu\nu\kappa\lambda]$ is Levi-Cevita tensor. If we impose the ideal MHD condition

$$u_\mu F^{\mu\nu} = 0, \tag{1.14}$$

which says that the Lorenz force vanishes in the rest frame of the fluid, the field tensor has only three independent components now. So it is convenient to describe the field by the magnetic field four-vector $\tilde{B}^\mu \equiv -n_\nu\ {}^*F^{\mu\nu}$. The vector $\tilde{B}^\mu$ differs from magnetic field variables as follows:

$$B^i \equiv\ {}^*F^{it} = \frac{\tilde{B}^i}{\alpha}. \tag{1.15}$$

We can define projection tensors

$$h_{\mu\nu} \equiv g_{\mu\nu} + u_\mu u_\nu, \tag{1.16}$$

which projects to the space perpendicular to four-velocity $u_\mu$ and

$$j_{\mu\nu} \equiv g_{\mu\nu} + n_\mu n_\nu, \tag{1.17}$$

which projects to the space perpendicular to normal observer's four-velocity $n^\mu$. The equations of GRMHD are :

$$T^\mu_{\nu;\mu} = 0, \tag{1.18}$$

which represents the conservation of energy-momentum tensor, the conservation of particle number

$$(\rho_0 u^\mu)_{;\mu} = 0 \tag{1.19}$$

and Maxwell's equations

$${}^*F^{\mu\nu}_{\ ;\nu} = 0. \tag{1.20}$$

For the gas we assume so called gamma law ($\Gamma$-law) with the equation of state

$$p = (\Gamma - 1)u. \tag{1.21}$$

Now we are going to investigate what should our energy-momentum tensor look like. First of all it is obvious that it consist of two parts

$$T^{\mu\nu} = T^{\mu\nu}_{fluid} + T^{\mu\nu}_{elmag}. \tag{1.22}$$

In a general meaning, the electromagnetic part of energy-momentum tensor is defined as follows

$$T^{\mu\nu}_{elmag} \equiv F^{\mu\lambda}F^\nu_\lambda - \frac{1}{4}g^{\mu\nu}F^{\lambda\delta}F_{\lambda\delta}. \tag{1.23}$$

This definition is valid for ${}^*F^{\mu\nu}$ too. For the dual of electromagnetic field tensor we can write ${}^*F^{\mu\nu} = (n^\mu \tilde{B}^\nu - n^\nu \tilde{B}^\mu)$. Now we can write for the electromagnetic part of the energy-momentum tensor following relation

$$\begin{aligned} T^{\mu\nu}_{elmag} = &\frac{(n^\mu \tilde{B}^\lambda - n^\lambda \tilde{B}^\mu)(n^\nu \tilde{B}_\lambda - n^\lambda \tilde{B}_\nu)(-n_\mu u^\mu)(-n_\nu u^\nu)}{\gamma \cdot \gamma} \\ &- \frac{1}{4}g^{\mu\nu}\frac{(n^\lambda \tilde{B}^\delta - n^\delta \tilde{B}^\lambda)(n_\lambda \tilde{B}_\delta - n_\delta \tilde{B}_\lambda)(-n_\lambda u^\lambda)(-n^\lambda u_\lambda)}{\gamma \cdot \gamma}, \end{aligned} \tag{1.24}$$

where we used the expression for the Lorenz factor of the flow measured in the normal observer's frame:

$$\gamma \equiv -n_\mu u^\mu. \tag{1.25}$$

There should be some constant, but it plays no role actually (the right hand side of the equation of conservation is zero), so we do not write it here. Using the identity $\tilde{B}^\mu n_\mu = 0$ we can rewrite the equation (1.24) to the form

$$T^{\mu\nu}_{elmag} = b^2 u^\mu u^\nu + \frac{1}{2}g^{\mu\nu}b^2 - b^\mu b^\nu, \tag{1.26}$$

where $b^\mu \equiv h^\mu{}_\nu \frac{\tilde{B}^\nu}{\gamma}$. For details see appendix (A1). For the energy-momentum tensor of ideal fluid we can write

$$T^{\mu\nu}_{fluid} = (\rho_0 + u + p)u^\mu u^\nu + pg^{\mu\nu} \tag{1.27}$$

and so the energy-momentum tensor has the form

$$T^{\mu\nu} = (w + b^2)u^\mu u^\nu + \left(p + \frac{b^2}{2}\right) g^{\mu\nu} - b^\mu b^\nu, \tag{1.28}$$

where $w \equiv \rho_0 + u + p$. Hereafter the primitive variables are: $\rho_0, u, \tilde{B}^i$ and $\tilde{u}^i \equiv j^i{}_\mu u^\mu$. The choice of $\tilde{u}^i$ is numerically convenient because it ranges from $-\infty$ to $+\infty$. Note that $\tilde{u}^t = 0$. We want to express conservation laws in terms of conserved variables $U$, fluxes $F$ and source terms $S$. It is easy to see that:

$$T^\mu{}_{\nu;\mu} = 0 \Rightarrow \frac{1}{\sqrt{-g}}(\sqrt{-g}T^\mu{}_\nu)_{,\mu} = -\Gamma_{\nu\rho\sigma}T^{\rho\sigma}. \tag{1.29}$$

It can be rewritten as

$$\partial_t(\sqrt{-g}T^t{}_\mu) + \partial_i(\sqrt{-g}T^i{}_\mu) = -\sqrt{-g}T^\kappa_\lambda \Gamma^\lambda{}_{\mu\kappa}. \tag{1.30}$$

The associated conserved variable is $\sqrt{-g}T^t{}_\mu$ but for the next purposes it is convenient to introduce a new conserved variable by

$$Q_\mu \equiv -n_\nu T^\nu{}_\mu = \alpha T^t{}_\mu, \tag{1.31}$$

which is the density of energy and momentum in the normal observer's frame. From the Maxwell's equations we get (note that ${}^*F^{\mu\nu} = \tilde{B}^\nu n^\mu - \tilde{B}^\mu n^\nu$)

$${}^*F^{0i}_{;i} = B^i{}_{;i} = 0, \tag{1.32}$$

which is the condition of zero magnetic field divergence and

$${}^*F^{i\mu}_{;\mu} = {}^*F^{i0}_{;0} + {}^*F^{ij}_{;j} = (n^i\tilde{B}^0 - n^0\tilde{B}^i)_{;0} + (n^i\tilde{B}^j - n^j\tilde{B}^i)_{;j} = 0. \tag{1.33}$$

From the last equation it follows that

$$\left(\frac{\tilde{B}^i}{\alpha}\right)_{;t} + (n^i\tilde{B}^j - n^j\tilde{B}^i)_{;j} = 0$$

and

$$\partial_t(\sqrt{-g}B^i) = -\partial_j[\sqrt{-g}(u^ib^j - u^jb^i)], \tag{1.34}$$

where we used $\tilde{B}^i = \gamma b^\mu h^i{}_\mu = \gamma b^i$ and $\gamma \equiv -n_\mu u^\mu = -n_t u^t$ (in normal observer's frame). Finally there is a particle number conservation law

$$\partial_t(\sqrt{-g}\rho_0 u^t) = -\partial_j(\sqrt{-g}\rho_0 u^j). \tag{1.35}$$

The conserved variable for this equation is $\sqrt{-g}\rho_0 u^t$, but as in the previous case it is convenient to introduce a new conserved variable defined by $D \equiv -\rho_0 n_\mu u^\mu = \rho_0 \alpha u^t = \gamma\rho_0$ which represents the mass density measured by the normal observer. So we have 8 conserved variables: $Q_\mu$,$D$ and $\tilde{B}^i$. The transformation $U(P)$ is already known:

$$p = (\Gamma - 1)u, \tag{1.36}$$

$$w = \rho_0 + u + p, \tag{1.37}$$

$$\gamma = (1 + g_{ij}\tilde{u}^i\tilde{u}^j), \tag{1.38}$$

$$u^\mu = \left(\frac{\gamma}{\alpha}, \tilde{u}^i - \alpha\gamma g^{ti}\right), \tag{1.39}$$

and

$$b^\mu = h^\mu{}_\nu \frac{\tilde{B}^\nu}{\gamma}. \tag{1.40}$$

Then we can evaluate $D$ and $Q_\mu$:

$$D = \gamma\rho_0, \tag{1.41}$$

$$Q_\mu = \gamma(w + b^2)u_\mu - \left(p + \frac{b^2}{2}\right) n_\mu + (n_\nu b^\nu) b_\mu. \tag{1.42}$$

$D$, $Q_\mu$ and $\tilde{B}^i$ are both conserved and primitive variables. Later in the paper it will be useful to use the identities

$$b^2 = \frac{1}{\gamma^2}[\tilde{B}^2 + (\tilde{B}^\mu u_\mu)^2] \tag{1.43}$$

and

$$n_\mu b^\mu = -u_\mu \tilde{B}^\mu. \tag{1.44}$$

So we have a system of five equations to be solved (one for $D$ and four for $Q_\mu$). Our approach to this problem is to evaluate some scalars from conserved variables to reduce the dimensionality of our system of equations. We will use $D$, $Q_\mu\tilde{B}^\mu$, $Q^\mu n_\mu$ and $\tilde{Q}^2$, where $\tilde{Q}^\nu \equiv j^\nu{}_\mu Q^\mu$. Moreover we will use $W \equiv w\gamma^2, v^i \equiv \frac{\tilde{u}^i}{\gamma}$. These new variables simplify the equations and lead to a more robust numerical scheme.

Now we evaluate our scalars (for details see (A2) and (A3) in appendix):

$$\tilde{B}^\mu Q_\mu = \frac{W}{\gamma}(u_\mu \tilde{B}^\mu), \tag{1.45}$$

$$Q_\mu n^\mu = -\frac{\tilde{B}^2}{2}(1 + v^2) + \frac{(\tilde{B}^\mu Q_\mu)^2}{2W^2} - W + p. \tag{1.46}$$

Now we evaluate $\tilde{Q}^2$. It is easy to show that

$$\tilde{Q}^\mu \tilde{Q}_\mu = (Q^\mu + n^\mu Q^\nu n_\nu) \cdot (Q_\mu + n_\mu n_\nu Q^\nu) = Q^2 + (n_\mu Q^\mu)^2. \tag{1.47}$$

We see that we must evaluate $(n_\mu Q^\mu)^2$ and $Q^2$. The first term we can get from (1.46) by simple multiplication

$$(n_\mu Q^\mu)^2 = \frac{\tilde{B}^4}{4}(1+v^2)^2 + \frac{(\tilde{B}^\mu Q_\mu)^4}{4W^4} + (p-W)^2 \\ - (1+v^2)\frac{\tilde{B}^2(\tilde{B}^\mu Q_\mu)^2}{2W^2} - \tilde{B}^2(1+v^2)(p-W) + \frac{(\tilde{B}Q_\mu)^2}{W^2}(p-W). \quad (1.48)$$

For $Q^2$ one can write

$$Q_\mu Q^\mu = -W^2(1-v^2) + 2Wp - p^2 + \tilde{B}^2\left(-\frac{W}{\gamma^2} + p(1+v^2) - \frac{(\tilde{B}^\mu Q_\mu)^2}{2W^2\gamma^2}\right) \\ + \frac{(\tilde{B}^\mu Q_\mu)^2\gamma^2}{W^2}\left(-\frac{W}{\gamma^2} + p(v^2-1)\right) - \frac{1}{4\gamma^4}\left(\tilde{B}^4 + \frac{(\tilde{B}^\mu Q_\mu)^4\gamma^4}{W^4}\right). \quad (1.49)$$

For details see (A4). Now if we put the expressions (1.49) and (1.48) into (1.47), we get

$$\tilde{Q}^2 = v^2(\tilde{B}^2+W)^2 - \frac{(Q_\mu\tilde{B}^\mu)^2(\tilde{B}^2+2W)}{W^2}. \quad (1.50)$$

From this equation we can express $v^2$

$$v^2 = \frac{\tilde{Q}^2W^2 + (Q_\mu\tilde{B}^\mu)^2(\tilde{B}^2+2W)}{(\tilde{B}^2+W)^2W^2}. \quad (1.51)$$

The $1D_W$ scheme solves one nonlinear algebraic equation (1.46), which is a function of $W$ since equation (1.51) is used to eliminate $v^2$. When we know $v^2$ and $W$ already, we can find $w, \rho_0$ and $u$.

Finally we need to find $\tilde{u}^i$. We use $\tilde{Q}^i$ for this purpose.

$$\tilde{Q}^\mu \equiv j^{\mu\nu}Q_\nu = \gamma(w+b^2)j^{\mu\nu}u_\nu + (n_\mu b^\mu)b_\nu j^{\mu\nu} \\ = \frac{1}{\gamma}(W+\tilde{B}^2)\tilde{u}^\mu + \frac{(\tilde{B}^\mu u_\mu)^2}{\gamma}u_\nu j^{\mu\nu} + (u_\mu\tilde{B}^\mu)^2 n^\mu - \frac{u_\mu\tilde{B}^\mu}{\gamma}h^\mu{}_\nu\tilde{B}^\nu \\ = \frac{1}{\gamma}(W+\tilde{B}^2)\tilde{u}^\mu - \frac{(u_\nu\tilde{B}^\nu)}{\gamma}\tilde{B}^\mu. \quad (1.52)$$

We can use the equation (1.45) to solve $\tilde{u}^i$:

$$\tilde{u}^i = \frac{\gamma}{W+\tilde{B}^2}\left(\tilde{Q}^i + \frac{(Q_\mu\tilde{B}^\mu)\tilde{B}^i}{W}\right). \quad (1.53)$$

The equation (1.46) which is solved in $1D_W$ scheme includes a quotient of polynomials in $W$. This can be the reason of some numerical pathologies near roots. A good approach to eliminating such problems is solving two simpler equations ( equation

(1.50) and equation (1.46) ) simultaneously for $W$ and $v^2$. This method is called the $2D$ scheme since it involves solving a two-dimensional algebraic system.

Using $v^2$ instead of $\tilde{u}^2$ or $\gamma$ is appropriate for this method because equations (1.50) and (1.46) are linear only in $v^2$ and not in $\tilde{u}^2$ or $\gamma$. The linear dependence on $v^2$ increases the rate of convergence for this quantity and is guaranteed to be well behaved in the vicinity of a root.

## 1.2 Numerical scheme

There are many possible ways to numerically integrate the GRMHD equations. The first choice which we can do is between conservative and nonconservative schemes. In the HARM the conservative scheme is applied. The advantage of this choice is that in one dimension total variation stable schemes are guaranteed to converge to a weak solution of the equations by the Lax-Wendroff theorem (Lax & Wendroff 1960) and by a theorem due to LeVeque (1997). While no such guarantee is available for multidimensional flows, this is a reassuring starting point. Furthermore, one is guaranteed that a conservative scheme in any number of dimensions will satisfy the jump conditions at discontinuities.

A conservative scheme updates a set of conserved variables at each time step. Our vector of conserved variables is

$$U \equiv \sqrt{-g}(\rho u^t, T^t_{\ t}, T^t_{\ i}, B^i). \tag{1.54}$$

These variables are updated using fluxes $F$. Also it is needed to choose a set of primitive variables, which are interpolated to model the flow within zones. We use variables with a simple physical interpretation:

$$P = (\rho, u, v^i, B^i), \tag{1.55}$$

where $v^i = \frac{u^i}{u^t}$ is the 3-velocity. The functions $U(P)$ and $F(P)$ are analytic, but the inverse operations are not. There is no simple expression for $F(U)$.

Since we update $U$ rather than $P$, we must solve $P(U)$ at the end of each time step. We use a multidimensional Newton-Raphson routine with the value of $P$ from the last time step as an initial guess. Since $B^i$ can be obtained analytically, only five equations need to be solved. The Newton-Raphson method requires an expensive evaluation of the Jacobian $\frac{\partial U}{\partial P}$. In practice we evaluate the Jacobian by numerical derivatives , but this is both expensive and a source of numerical noise.

The evaluation of $P(U)$ is the crucial point of our numerical scheme. To evaluate $F$, we use a MUSCL-type scheme with "HLL" fluxes (Harten et al. 1983). The fluxes are defined at zone faces. A slope-limited linear extrapolation from the zone center gives $P_R$ and $P_L$, the primitive variables at the right and left-hand side of each zone interface. The monotonized central limiter, the van Leer limiter and the minmod limiter are implemented in HARM.

In general a system of conservation laws with some extra source terms can be written as

$$\partial_t U + \partial_i F^i(U) = S(U), \tag{1.56}$$

where $U$,$F$ and $S$ are vectors of conserved variables, fluxes and source terms. $\partial_i$ represents the spatial derivative in direction $i$ and the summation is implied over $i = 1, 2, 3$. In following text we closely follow Tóth (1998).

## TVD Lax-Friedrichs scheme

Some of the most popular methods for solving a hyperbolic system of PDE are the total variation diminishing (TVD) type schemes. Although these schemes were developed and used for compressible hydrodynamics, their application to MHD is relatively recent. There are several variations and generalizations of TVD schemes, like total variation bounded (TVB), essentially non-oscillatory (ENO) etc. methods, but these are not discussed here. Even within the TVD family there are dozens of variants, therefore we concentrate on the simplest versions. The simplest TVD type scheme is based on the first order Lax-Friedrichs scheme, which discretizes a conservation law according to

$$U_j^{n+1} = U_j^n - \frac{\Delta t}{\Delta x}\left(F_{j+\frac{1}{2}} - F_{j-\frac{1}{2}}\right) + \frac{1}{2}\left(\phi_{j+\frac{1}{2}} - \phi_{j-\frac{1}{2}}\right), \tag{1.57}$$

where

$$F_{j+\frac{1}{2}} = \frac{F_j + F_{j+1}}{2} \tag{1.58}$$

and

$$\phi_{j+\frac{1}{2}} = U_{j+1} - U_j. \tag{1.59}$$

The last two terms in (1.57) add numerical diffusion which corresponds to a term of the form $\eta\nabla^2 U$ with the diffusion coefficient $\eta \propto \frac{(\Delta x)^2}{\Delta t}$. So the Lax-Friedrichs scheme is only first order accurate. One can also show that the scheme is conditionally stable for Courant number $C < 1$. The numerical diffusion can be reduced by using a diffusive flux

$$\phi_{j+\frac{1}{2}} = \frac{\Delta t}{\Delta x} c^{max}_{j+\frac{1}{2}}(U_{j+1} - U_j), \tag{1.60}$$

where the local Courant number $C = c^{max}\frac{\Delta t}{\Delta x}$ ($c^{max}$ denotes the fastest wave speed) is used as a coefficient for the artificial diffusion. The scheme we have just described is the first order TVD Lax-Friedrichs scheme.

Another way to look at the numerical flux terms $\phi$ is to realize that they modify the centered flux difference formula to a one-sided upwinded difference formula, at least for a single linear equation like the continuity equation $\frac{\partial \rho}{\partial t} + \nabla \cdot (\rho v) = 0$. For a fixed velocity, the maximum wave speed is $c^{max} = |v|$, and we can write

$$\rho_j^{n+1} = \rho_j^n - \frac{\Delta t}{2\Delta x}[(\rho v)_{j+1} - (\rho v)_{j-1}] + \frac{\Delta t}{2\Delta x}|v|(\rho_{j+1} - 2\rho_j + \rho_{j-1})$$

$$= \rho_j^n - \frac{\Delta t}{\Delta x} \begin{cases} (\rho v)_j - (\rho v)_{j-1} & \text{for } v \geq 0 \\ (\rho v)_{j+1} - (\rho v)_j & \text{for } v < 0. \end{cases} \tag{1.61}$$

The upwinded difference formula is very appropriate for the advection equation, and in general for hyperbolic equations, since physical information should propagate from the upstream direction.

Second order spatial accuracy can be achieved by a linear approximation of $U$ and the corresponding fluxes at the boundary interfaces. The value of $U$ at the interface at $x_{j+\frac{1}{2}}$ can be linearly extrapolated from the left and right cell center values as

$$U^L_{j+\frac{1}{2}} = U^n_j + \frac{1}{2}\overline{\Delta U}^n_j$$

and

$$U^R_{j+\frac{1}{2}} = U^n_{j+1} - \frac{1}{2}\overline{\Delta U}^n_{j+1}, \tag{1.62}$$

where the limited slopes $\overline{\Delta U}$ will be defined later. The fluxes at the cell interface are calculated as

$$F_{j+\frac{1}{2}} = \frac{F(U^L_{j+\frac{1}{2}}) + F(U^R_{j+\frac{1}{2}})}{2}, \tag{1.63}$$

$$\phi_{j+\frac{1}{2}} = \frac{\Delta t}{\Delta x} c^{max}_{j+\frac{1}{2}} \left( U^R_{j+\frac{1}{2}} - U^L_{j+\frac{1}{2}} \right). \tag{1.64}$$

The diffusive flux $\phi$ has been reduced since the difference between the left and right extrapolation is proportional to $(\Delta x)^2$ for a smoothly varying $U$. It still provides proper upwinding for the flux difference formula. The maximum propagation speed can be defined as $c^{max}_{j+\frac{1}{2}} = max[c^{max}(U^R), c^{max}(U^L)]$.

For explicit time stepping, temporally second order accuracy can be achieved by some two step Runge-Kutta discretization, or a predictor-corrector scheme. Hancock's predictor step is probably the best choice. First a time centered

$$U^{n+\frac{1}{2}}_j = U^n_j - \frac{\Delta t}{2\Delta x} \left[ F(U^n_j + \frac{1}{2}\overline{\Delta U}^n_j) - F(U^n_j - \frac{1}{2}\overline{\Delta U}^n_j) \right] \tag{1.65}$$

is calculated and then it is used for calculating the linear extrapolations

$$U^L_{j+\frac{1}{2}} = U^{n+\frac{1}{2}}_j + \frac{1}{2}\overline{\Delta U}^n_j$$

and

$$U^R_{j+\frac{1}{2}} = U^{n+\frac{1}{2}}_{j+1} - \frac{1}{2}\overline{\Delta U}^n_{j+1}. \tag{1.66}$$

This is a spatially and temporally second order TVDLF scheme which is stable for Courant number $C < 1$. Contributions of source terms can be added easily to the right hand side of (1.65). In multidimensional simulations the $U^L$ and $U^R$ extrapolations should be determined for each interface, and the flux contributions can be added at the same time, however this usually requires the Courant number

to be reduced to about $C < 0.5$.

## TVD-MUSCL scheme

The TVD-MUSCL scheme (MUSCL means the Monotonic Upstream Scheme for Conservation Laws) differs from the TVDLF scheme in that the upwinding is applied for characteristic variables rather than the conserved variables. The characteristic variables $\vec{r}^k$ are certain linear combination of the conserved variables that form the right eigenvectors of the matrix $\frac{\partial \vec{F}}{\partial \vec{U}}$, ie.

$$\frac{\partial \vec{F}}{\partial \vec{U}} \vec{r}^k = c^k \vec{r}^k, \tag{1.67}$$

where $c^k$ is the eigenvalue corresponding to the $k$-th eigenvector. For a linear system of hyperbolic PDE-s, the characteristic waves consist of components $\vec{r}^k$ that travel at a speed $c^k$. Hyperbolicity ensures that the eigenvectors and eigenvalues are real and a complete orthogonal basis can be formed from them. The normalized left eigenvectors $\vec{l}^k$ are related to the right eigenvectors by the orthogonality relation $\vec{l}^k \cdot \vec{r}^m = \delta_{k,m}$.
Now we can modify the numerical diffusive flux vector $\vec{\phi}$ to be

$$\vec{\phi} = \frac{\Delta t}{\Delta x} \sum_k \vec{r}^k |c^k| \vec{l}^k \cdot (\vec{U}^R - \vec{U}^L), \tag{1.68}$$

where $\vec{r}^k$, $c^k$, $\vec{l}^k$ are calculated for the averaged $U^{LR}_{j+\frac{1}{2}}$ state. The scalar product of the $k$-th left eigenvector with $\vec{U}^R - \vec{U}^L$ determines the jump in the $k$-th characteristic variable, while the multiplication by $\vec{r}^k$ transforms the result back to the conserved variables. The gain relative to the much simpler TVDLF flux is the use of the eigenvalue $c^k$ instead of the largest eigenvalue $c^{max}$. Therefore the upwinding is accurate for each characteristic variable, which means less numerical diffusion. On the other hand, the left and right eigenvectors need to be calculated for each cell interface, which is rather expensive for the GRMHD equations.

## Slope limiters

In the second order TVDLF and TVD-MUSCL schemes the $\Delta U$ slopes of the conserved variables are limited by slope limiters denoted by $\overline{\Delta U}$. The slope limiter is required to ensure the TVD property for the schemes. There are many versions of slope limiters that satisfy both conditions for TVD property and second order accuracy for smooth solutions. Here we define only three: the minmod limiter, the van Leer limiter and superbee limiter. In our computation we use the van Leer

limiter which is defined by

$$\overline{\Delta U_j} = minmod(2\Delta U_{j-\frac{1}{2}}, 2\Delta U_{j+\frac{1}{2}}, \frac{1}{2}\Delta U_{j-\frac{1}{2}} + \frac{1}{2}\Delta U_{j+\frac{1}{2}}). \tag{1.69}$$

The minmod limiter is defined as

$$\overline{\Delta U_j} = minmod(\Delta U_{j-\frac{1}{2}}, \Delta U_{j+\frac{1}{2}}) \tag{1.70}$$

and the superbee limiter by

$$\overline{\Delta U_j} = s\ max[0, min(2|\Delta U_{j+\frac{1}{2}}|, s\Delta U_{j-\frac{1}{2}}), min(|\Delta U_{j+\frac{1}{2}}|, 2s\Delta U_{j-\frac{1}{2}})], \tag{1.71}$$

where $\Delta U_{j+\frac{1}{2}} = U_{j+1} - U_j$, $s = sgn(\Delta U_{j+\frac{1}{2}})$ and generalized minmod function for argument $n > 1$ is defined as

$$minmod(w_1, w_2, ..., w_n) \equiv sgn(w_1)max[0, min(|w_1|, sgn(w_1)w_2, ..., sgn(w_1)w_n)]. \tag{1.72}$$

The definition of minmod function means that it takes the argument with the smallest modulus when all arguments have the same signs and otherwise it is zero. The minmod limiter is rather diffusive, while the superbee limiter can sharpen smooth waves into discontinuities. In fact, the minmod and the superbee limiters are the most and least diffusive of all acceptable symmetric two-variable slope limiters. The van Leer limiter is between those two and it is often used as a good compromise.

# 2. Fluid tori orbiting Kerr black hole

## 2.1 Fishbone-Moncrief model of accretion torus: $l_* = const.$

The Fishbone-Moncrief torus (Fishbone & Moncrief 1976) is a model of a fluid torus orbiting Kerr Black Hole. The spacetime can be expressed by

$$ds^2 = -e^{2\nu}\mathrm{d}t^2 + e^{2\psi}(\mathrm{d}\varphi - \omega\mathrm{d}t)^2 + e^{2\lambda}\mathrm{d}r^2 + e^{2\mu}\mathrm{d}\Theta^2, \tag{2.1}$$

where $\nu, \psi, \omega, \lambda, \mu$ are functions of $r$ and $\Theta$. Four-velocity of the fluid $u^\alpha$ satisfies:

a) $u^r = u^\Theta = 0$,

b) $g_{\alpha\beta}u^\alpha u^\beta = -1$

and

c)$u^t$, $u^\varphi$ are functions of $r$ and $\Theta$ only.

We are interested in thermodynamical functions such as $p, \rho$, baryon number density $n$, entropy per baryon $s$, temperature $T$ and enthalpy per baryon $h$ which satisfies

$$h = \frac{p+\rho}{n} \tag{2.2}$$

and

$$\mathrm{d}p = n\mathrm{d}h - nT\mathrm{d}s. \tag{2.3}$$

The Euler equations follows from energy-momentum tensor conservation

$$T^{\alpha\beta}_{\ ;\beta} = 0, \tag{2.4}$$

where

$$T^{\alpha\beta} = (p+\rho)u^\alpha u^\beta + pg^{\alpha\beta}. \tag{2.5}$$

One more equation we can obtain from the baryon number conservation law

$$(nu^\alpha)_{;\alpha} = 0. \tag{2.6}$$

The Euler equations (2.4) reduces to

$$\mathrm{d}[\ln h + \nu] - \left(\frac{T}{h}\right)\mathrm{d}s = {u_{(\varphi)}}^2\mathrm{d}(\psi - \nu) - u_{(\varphi)}[1 + {u_{(\varphi)}}^2]^{\frac{1}{2}}e^{\psi-\nu}\mathrm{d}\omega, \tag{2.7}$$

where

$$u_{(\varphi)} = e^{-\psi}u_\varphi$$

and

$$u_{(t)} = -[1 + (u_{(\varphi)})^2]^{\frac{1}{2}} = e^{-\nu}(u_t + \omega u_\varphi) \tag{2.8}$$

are projections of four-velocity $u^\alpha$ onto orthonormal vectors of locally nonrotating frame (Bardeen et al. 1972) defined by

$$e_{(t)} = e^{-\nu}\left(\frac{\partial}{\partial t} + \omega\frac{\partial}{\partial\varphi}\right),\ e_{(\varphi)} = e^{-\psi}\frac{\partial}{\partial\varphi},$$

$$e_{(r)} = e^{-\lambda}\frac{\partial}{\partial r},\ e_{(\Theta)} = e^{-\mu}\frac{\partial}{\partial\Theta}. \tag{2.9}$$

We are interested only in cases for which $\mathrm{d}s = 0$. Defining $\chi \equiv \psi - \nu$ and $\phi \equiv \ln h + \nu$, the equation (2.7) reduces to

$$\mathrm{d}\phi \equiv \mathrm{d}[\ln h + \nu] = (u_{(\varphi)})^2\mathrm{d}\chi - u_{(\varphi)}[1 + (u_{(\varphi)})^2]^{\frac{1}{2}}e^{\chi}\mathrm{d}\omega. \tag{2.10}$$

We can see that $\phi$ must always be expressible purely as a function of $\chi$ and $\omega$. Let's suppose first that $\chi$ and $\omega$ are independent variables. Then from the equation (2.10) it follows that

$$\frac{\partial\phi}{\partial\chi} = (u_{(\varphi)})^2$$

and

$$\frac{\partial\phi}{\partial\omega} = -u_{(\varphi)}[1 + (u_{(\varphi)})^2]^{\frac{1}{2}}e^{\chi}, \tag{2.11}$$

which implies a relationship between $\frac{\partial\phi}{\partial\chi}$ and $\frac{\partial\phi}{\partial\omega}$, which we obtain by eliminating $u_{(\varphi)}$ from these expressions. If $\chi$ and $\omega$ are linearly dependent in some region then equations (2.11) do not follow from equation (2.10). But we can impose these equations as a means of eliminating the lack of uniqueness in the representation of $\phi$ as a function of $\chi$ and $\omega$. If $\chi$ and $\omega$ are linearly dependent functions of $r$ and $\Theta$, the representation of $\phi = \phi(\chi, \omega)$ is not unique since we can reexpress $\omega$ in terms of $\chi$ or vice versa. This convention is very useful because if we adopt it we can treat both dependent and independent cases in the same way. From equation (2.11) we get Hamilton-Jacobi differential equation for $\phi(\chi, \omega)$

$$-\frac{\partial\phi}{\partial\omega} = \left[\frac{\partial\phi}{\partial\chi}\left(1 + \frac{\partial\phi}{\partial\chi}\right)\right]^{\frac{1}{2}}e^{\chi}. \tag{2.12}$$

We took a positive sign in the expression $u_{(\varphi)} = \pm\left(\frac{\partial\phi}{\partial\chi}\right)^{\frac{1}{2}}$. Solution for the negative choice could be generated by replacing $\omega$ with $(-\omega)$. If we view $\chi$ as a canonical coordinate and $\omega$ as the time, then equation (2.12) is the Hamilton-Jacobi equation for the time-independent Hamiltonian

$$H(\chi, \Pi) = [\Pi(1 + \Pi)]^{\frac{1}{2}}e^{\chi}, \tag{2.13}$$

where $\Pi$ is the momentum conjugate to $\chi$. The solutions of Hamilton's equations are

$$\frac{\mathrm{d}\chi}{\mathrm{d}\omega} = \frac{\partial H}{\partial\Pi} = \frac{e^{\chi}}{2}\left[\left(\frac{1+\Pi}{\Pi}\right)^{\frac{1}{2}} + \left(\frac{\Pi}{1+\Pi}\right)^{\frac{1}{2}}\right]$$

and

$$\frac{\mathrm{d}\Pi}{\mathrm{d}\omega} = -\frac{\partial H}{\partial \chi} = -H. \tag{2.14}$$

Let $\chi_0$ and $\Pi_0$ be the initial values of $\chi$ and $\Pi$ at time $\omega = \omega_0$ and set

$$H_0 = H(\chi_0, \Pi_0). \tag{2.15}$$

Since $H$ is conserved one can write

$$H(\chi(\omega), \Pi(\omega)) = H(\chi_0, \Pi_0) \tag{2.16}$$

and equation (2.14) gives

$$\Pi(\omega) = \Pi_0 - (\omega - \omega_0)H_0. \tag{2.17}$$

When we put equations (2.13),(2.16) and (2.17) together, we obtain

$$e^{-\chi(\omega)} = e^{-\chi_0}\left[\frac{\Pi_0 - (\omega-\omega_0)H_0}{\Pi_0}\right]^{\frac{1}{2}}\left[\frac{1+\Pi_0-(\omega-\omega_0)H_0}{1+\Pi_0}\right]^{\frac{1}{2}}, \tag{2.18}$$

which, together with equation (2.17), provides the general solution of Hamilton's equations. Along a characteristic curve (it means the solution of Hamilton's equations) $\phi$ obeys

$$\begin{aligned}\frac{\mathrm{d}\phi}{\mathrm{d}\omega} &= \frac{\partial\phi}{\partial\chi}\frac{\mathrm{d}\chi}{\mathrm{d}\omega} + \frac{\partial\phi}{\partial\omega} \\ &= \Pi\frac{\mathrm{d}\chi}{\mathrm{d}\omega} - H(\chi,\Pi).\end{aligned} \tag{2.19}$$

We will integrate equation (2.19) along the characteristic curves to determine $\phi$ as a function of $\chi$ and $\omega$. Letting $\phi_0(\chi_0) = \phi(\chi_0, \omega_0)$ represent the values of $\phi$ at initial points $(\chi_0, \omega_0)$, we have for the initial momentum

$$\Pi_0(\chi_0) = \frac{\mathrm{d}\phi_0}{\mathrm{d}\chi_0} \equiv {\phi_0}'. \tag{2.20}$$

Moreover we can write thanks to equations (2.13),(2.17),(2.18) and (2.20)

$$\Pi(\chi_0, \omega) = {\phi_0}' - (\omega-\omega_0)e^{\chi_0}[{\phi_0}'(1+{\phi_0}')]^{\frac{1}{2}} \tag{2.21}$$

and

$$\begin{aligned}\exp[-\chi(\chi_0,\omega)] = e^{-\chi_0}&\left[1-(\omega-\omega_0)e^{\chi_0}\left(\frac{1+{\phi_0}'}{{\phi_0}'}\right)^{\frac{1}{2}}\right]^{\frac{1}{2}}\cdot \\ &\cdot\left[1-(\omega-\omega_0)e^{\chi_0}\left(\frac{{\phi_0}'}{1+{\phi_0}'}\right)^{\frac{1}{2}}\right]^{\frac{1}{2}}.\end{aligned} \tag{2.22}$$

Along the characteristic curve we get from the equation (2.19):

$$\frac{\mathrm{d}\phi}{\mathrm{d}\omega} = \Pi\frac{\mathrm{d}\chi}{\mathrm{d}\omega} - H(\chi,\Pi) = -\frac{H(\chi,\Pi)}{2(1+\Pi)}, \tag{2.23}$$

where we have used Hamilton's equation for $\frac{\mathrm{d}\chi}{\mathrm{d}\omega}$. Since $H$ is conserved and $\Pi$ depends linearly on time along characteristics, we can easily integrate equation (2.23) and get

$$\phi(\chi,\omega) = \phi_0(\chi_0) + \frac{1}{2}\ln\left(1 - (\omega-\omega_0)e^{\chi_0}\left[\frac{{\phi_0}'(\chi_0)}{1+{\phi_0}'(\chi_0)}\right]^{\frac{1}{2}}\right). \tag{2.24}$$

Equations (2.24) and (2.22) constitute a parametrized form of the general solution to the Hamilton-Jacobi form of Euler's equations. Another important view to our problem can be gained from equations (2.11) and (2.12), because from these two equations it follows that the Hamiltonian $H$ can be expressed in the form

$$H = u_\varphi[1+(u_\varphi)^2]^{\frac{1}{2}}e^{\chi} = -u_{(\varphi)}u_{(t)}e^{\chi} = u_\varphi u^t, \tag{2.25}$$

where we have used equations (2.8) and the inverse metric $g^{\mu\nu}$. Killing equations for the vector field $\xi = \frac{\partial}{\partial\varphi}$ combined with Euler equations $T^{\alpha\beta}_{\ \ ;\beta} = 0$ imply the conservation of the flow of angular momentum

$$L_z = \int\sqrt{-g}\xi_\mu T^{\mu t}\mathrm{d}^3x = \int\sqrt{-g}(p+\rho)u_\varphi u^t\mathrm{d}^3x, \tag{2.26}$$

where we integrate over entire volume of the fluid in a $t = const.$ hypersurface. It is natural to call the value $\sqrt{-g}(p+\rho)$ the density of inertial mass. Then from the equations (2.25) and (2.26) it is easy to see that $H = u_\phi u^t$ is the flow of angular momentum per unit inertial mass. Since $H$ is a constant of motion (Hamiltonian which is not explicitly dependent on time is always constant of motion thanks to Poisson brackets identity) we are going to assume $H$ to be a constant throughout entire volume of a torus. We want to find a solution of equation (2.10). We will use an identity

$$(u_{(\varphi)})^2 = \frac{\partial\phi}{\partial\chi} = \frac{-1+(1+4l^2e^{-2\chi})^{\frac{1}{2}}}{2}, \tag{2.27}$$

where we have used equations (2.11),(2.13), (2.25) and the definition $l \equiv u_\varphi u^t$. Then, after integrating we get

$$\phi(\chi,\omega) \equiv \ln h + \nu = \frac{1}{2}\ln[1+(1+4l^2e^{-2\chi})^{\frac{1}{2}}] - \frac{1}{2}(1+4l^2e^{-2\chi})^{\frac{1}{2}} - l\omega + \phi_{in}, \tag{2.28}$$

where $\phi_{in}$ is a constant. Now we are going to specify solution (2.28) to the Kerr background gravitational field. The appropriate metric functions are

$$e^{2\nu} = \frac{\Sigma\Delta}{A},\ e^{2\psi} = \frac{A\sin\vartheta^2}{\Sigma},\ \omega = \frac{2aMr}{A}, \tag{2.29}$$

where

$$\Delta \equiv r^2 - 2Mr + a^2,$$
$$\Sigma \equiv r^2 + a^2 \cos\vartheta^2,$$
$$A \equiv (r^2 + a^2)^2 - \Delta a^2 \sin\vartheta^2. \tag{2.30}$$

The solution (2.28) now becomes

$$\begin{aligned}\ln h = {} & \frac{1}{2}\ln\left(\frac{1+[1+4l^2\Sigma^2\Delta(A\sin\vartheta)^{-2}]^{\frac{1}{2}}}{\Sigma\Delta A^{-1}}\right) - \frac{1}{2}\left[1+\frac{4l^2\Sigma^2\Delta}{(A\sin\vartheta)^2}\right]^{\frac{1}{2}} - \frac{2aMrl}{A} \\ & - \frac{1}{2}\ln\left(\frac{1+[1+4l^2{r_{in}}^2({r_{in}}^2-2Mr_{in}+a^2)({r_{in}}^3+r_{in}a^2+2Ma^2)^{-2}]^{\frac{1}{2}}}{r_{in}({r_{in}}^2-2Mr_{in}+a^2)({r_{in}}^3+r_{in}a^2+2Ma^2)^{-1}}\right) \\ & + \frac{1}{2}\left[1+\frac{4l^2{r_{in}}^2({r_{in}}^2-2Mr_{in}+a^2)}{({r_{in}}^3+r_{in}a^2+2Ma^2)^2}\right]^{\frac{1}{2}} + l\left[\frac{2aM}{({r_{in}}^3+r_{in}a^2+2Ma^2)}\right]. \end{aligned} \tag{2.31}$$

The last three terms in this equation are the negatives of the first three evaluated at the point $r = r_{in}$, $\vartheta = \frac{\Pi}{2}$. For the equations of state which we consider here, the tori would consist of a region of positive values of $\ln h$ bounded by a surface at which $\ln h = 0$. To show that such tori exist, it is necessary to investigate the qualitative behavior of the $\ln h$ expression. We can limit this investigation to the values of $\ln h$ on the equatorial plane, because the dependence on $\vartheta$ is simple to understand. As $\vartheta \to 0$ or $\Pi$, $\sin\vartheta \to 0$, the dominant behavior in this limit occurs through the second term in expression (2.31). This leads to a large negative contribution to $\ln h$ and causes any otherwise acceptable torus (for which $\ln h > 0$ at $\vartheta = \frac{\Pi}{2}$) to be bounded by some nonzero value of $\vartheta$.

That $\ln h$ depends only on $\sin^2\vartheta$ in a sufficiently regular way also means that the inner and outer surfaces of any torus will have no cusps at the equator. This follows by taking the derivative with respect to $\vartheta$ of the boundary-defining equation $\ln h(r,\vartheta) = 0$. The resulting equation has the form $\frac{\mathrm{d}r}{\mathrm{d}\vartheta} = \cos\vartheta \cdot g(r,\vartheta)$, where $g$ is some complicated function that is, nevertheless, regular at $\vartheta = \frac{\Pi}{2}$. Thus $\frac{\mathrm{d}r}{\mathrm{d}\vartheta} = 0$ at $\frac{\Pi}{2}$, so the boundary is smooth where it crosses the equator.

From the inner boundary of a torus at $r = r_{in}$, $\ln h$ must increase from zero (since this corresponds to increasing pressure), reach a maximum at a radius where pressure-gradient forces vanish and where the flow is geodesic and finally decrease to zero at the outer boundary. Whether $\ln h$ increases or decreases from zero and whether or not it finally decreases to zero depends on the value of the constant $l$. If $l$ is too small, $\ln h$ will decrease as $r$ increases from $r_{in}$, while if $l$ is too large, $\ln h$ will not return to zero for any $r > r_{in}$. Neither of these facts is simple to ascertain in the complete generality of the Kerr metric.

We are interested here in the case where $[\ln h(r, \frac{\Pi}{2})]_{,r} = 0$. A useful expression is

$$\left[\ln h\left(r,\frac{\Pi}{2}\right)\right]_{,r} = -\frac{1}{2}(\psi+\nu)_{,r} - l\omega_{,r} + \frac{1}{2}\chi_{,r}(1+4l^2e^{-2\chi})^{\frac{1}{2}}. \tag{2.32}$$

By equating this expression to zero, we find after some algebraic manipulation that

$$l = l(r) \equiv \pm \left(\frac{M}{r^3}\right)^{\frac{1}{2}} \left[\frac{r^4 + r^2a^2 - 2Mra^2 \mp a(Mr)^{\frac{1}{2}}(r^2 - a^2)}{r^2 - 3Mr \pm 2a(Mr)^{\frac{1}{2}}}\right]. \tag{2.33}$$

Now we can construct the torus of $l = const.$ by evaluating $l$ at some radius (which will be the point of maximal pressure according to the fact that $[\ln h(r, \frac{\Pi}{2})]_{,r} = 0$ for $l$ obtained from (2.33)).

## 2.2 Abramowicz et al.model of accretion torus: *l=const.*

In this section I provide a short introduction to the relativistic von Zeipel's theorem at first, because I will refer to it later. The general relativistic von Zeipel's theorem (Abramowicz 1971) tells us about the sufficient and necessary condition for the coincidence of isobaric and equidensity surfaces in the interior of an isolated, axially symmetric rotating mass of a perfect fluid in a steady state ("star"). We adopt following assumptions:

a) The spacetime manifold of the star is asymptotically flat at radial infinity.

b) The star and its manifold are stationary, and so a Killing vector field $\eta$ (which is timelike at radial infinity and has a unit lenght) exists there.

c) The star and its manifold are axially symmetric, so that there exists a Killing vector field $\xi$, which is spacelike at radial infinity and furthermore it is orthogonal to $\eta$.

d) The star is made of a perfect fluid, which rotates only in the $\xi$ direction so that

$$\mathcal{L}_\xi u = 0, \tag{2.34}$$

where $\mathcal{L}$ denotes the Lie derivative and $u$ denotes the four-velocity of the fluid.

We call the object satisfying properties a),...,d) the star. For the rotating star we have

$$\xi^\mu p_{,\mu} = \eta^\mu p_{,\mu} = u^\mu p_\mu = 0, \tag{2.35}$$

where coma denotes the partial derivative. We want to show that following theorems are valid:

1) The surfaces of constant density of angular momentum per unit inertial mass $l(r, \vartheta)$ and the surfaces of constant angular velocity of rotation $\Omega(r, \vartheta)$ coincide with each other in the interior of the rotating star if and only if the star is barotropic:

$$p = p(\rho_0) \Leftrightarrow F(l, \Omega) = 0. \tag{2.36}$$

2) The surfaces of constant density of angular momentum per baryon $j$ and the surfaces of constant angular velocity of rotation $\Omega$ coincide in the interior of the rotating star if the star is isentropic:

$$\sigma_{,\mu} = 0 \Rightarrow F(j, \Omega) = 0. \tag{2.37}$$

*Proof.* We will use a coordinate system in which

$$\eta^\mu = \delta^\mu_t, \tag{2.38}$$

$$\xi_\mu = \delta^\mu_\varphi \tag{2.39}$$

and

$$ds^2 = g_{tt}dt^2 + 2g_{t\varphi}d\varphi dt + g_{\varphi\varphi}d\varphi^2 + g_{AB}dx^A dx^B, \tag{2.40}$$

where A=1,2 and B=1,2. In this coordinate system we have following expressions for angular velocity of rotation, density of angular momentum per baryon and density of angular momentum per unit inertial mass:

$$\Omega = \frac{u^\varphi}{u^t} = \frac{d\varphi}{dt}, \tag{2.41}$$

$$j = \frac{p+\rho_0}{n}u_\varphi, \tag{2.42}$$

$$l = \frac{u_\varphi}{u_t}. \tag{2.43}$$

$n$ denotes the density of baryon number. It is not difficult to show that the equations of energy-momentum tensor conservation, $T^\mu_{\nu;\mu} = 0$, for a hydrodynamical case of tensor

$$T_{\mu\nu} = (p+\rho_0)u_\mu u_\nu + pg_{\mu\nu} \tag{2.44}$$

can be put into the form

$$(p+\rho_0)u^\nu u_{\mu;\nu} = -p_{,\mu} - u_\mu u^\nu p_{,\nu}. \tag{2.45}$$

We will use following expressions to rewrite the last equation.

$$u^\nu u_{\mu;\nu} = -u^\nu \Gamma^\sigma_{\mu\nu}u_\sigma = -\frac{1}{2}g_{\nu\rho,\mu}u^\nu u^\rho, \tag{2.46}$$

$$g_{\nu\rho}u^\nu u^\rho = -1 \Rightarrow (g_{\nu\rho}u^\nu u^\rho)_{,\mu} = 0, \tag{2.47}$$

which implies that

$$g_{\nu\rho,\mu}u^\nu u^\rho = -g_{\nu\rho}(u^\nu_{,\mu}u^\rho + u^\nu u^\rho_{,\mu}). \tag{2.48}$$

If we put the last three equations together we will get

$$u^\nu u_{\mu;\nu} = \frac{1}{2}(u^\nu_{,\mu}u_\nu + u_\rho u^\rho_{,\mu}) = u_t u^t_{,\mu} + u_\varphi u^\varphi_{,\mu}. \tag{2.49}$$

Thanks to the fact that $u^\mu p_{,\mu} = 0$, we have

$$\begin{aligned}(p+\rho_0)^{-1}p_{,\mu} &= -u_t u^t_{,\mu} - u_\varphi u^\varphi_{,\mu} = -u_\varphi u^\varphi_{,\mu} - \frac{u_t u^t u^t_{,\mu} + u^t_{,\mu} - u^t_{,\mu}}{u^t} \\ &= \frac{u^t_{,\mu}}{u^t} - \frac{u^t u_\varphi u^t u^\varphi_{,\mu} - u^t u^\varphi u_\varphi u^t_\mu}{(u^t)^2} \\ &= (\ln u^t)_{,\mu} - (u^t u_\varphi)\Omega_{,\mu}.\end{aligned} \tag{2.50}$$

Now we apply the covariant derivative on this equation and furthermore we multiply the result of this operation by the completely antisymmetric tensor $\epsilon^{\kappa\lambda\mu\nu}$. Then we obtain:

$$(p+\rho_0)^{-2}\rho_{0,\nu}p_{,\mu}\epsilon^{\kappa\lambda\mu\nu} = (u^t u_\varphi)_{,\nu}\Omega_{,\mu}\epsilon^{\kappa\lambda\mu\nu}. \tag{2.51}$$

From the last two equations we see that in the case of the rigid rotation ($\Omega_{,\mu} = 0$) the gradients of $\rho_0$, $p$ and $u^t$ are parallel and so the surfaces of their constant values must coincide. From equation (2.51) it follows that the gradients of density and pressure are parallel if and only if

$$(u^t u_\varphi)_{,\nu}\Omega_{,\mu}\epsilon^{\kappa\lambda\mu\nu} = 0, \tag{2.52}$$

or equivalently written in another form

$$f(u^t u_\varphi, \Omega) = 0, \tag{2.53}$$

where $f$ is a function of $\Omega$ and $u^t u_\varphi$ only. From the normalization condition for four-velocity we obtain

$$u^t u_\varphi = -(\Omega + l^{-1})^{-1} \tag{2.54}$$

and

$$F(l, \Omega) = 0 \tag{2.55}$$

as a result of equations (2.54) and (2.53). One can see that we have just proven a statement (2.36). □

I will not demonstrate the proof of the second statement here.

## Relativistic concept of angular momentum density

The most frequently used definitions of angular momentum density in a relativistic case are:

$$l = -\frac{u_\varphi}{u_t}, \tag{2.56}$$

$$l_0 = -u_\varphi, \tag{2.57}$$

$$l_* = -u_\varphi u^t. \tag{2.58}$$

The relativistic angular momentum velocity is defined by

$$\Omega = \frac{u^\varphi}{u^t}. \tag{2.59}$$

From the expressions (2.56) and (2.59) it follows that

$$l = -\frac{g_{t\varphi} + \Omega g_{\varphi\varphi}}{g_{tt} + \Omega g_{t\varphi}}$$

and

$$\Omega = -\frac{g_{t\varphi} + l g_{tt}}{g_{\varphi\varphi} + l g_{t\varphi}}. \tag{2.60}$$

We will call the surfaces of constant $l$ and $\Omega$ the von Zeipel's cylinders. If the background gravitational field is known and a special form of the von Zeipel's formula is assumed one can easily find the explicit form of the functions

$$l = l(r, \theta)$$

and

$$\Omega = \Omega(r, \theta) \tag{2.61}$$

by solving equation (2.60).

In the barotropic case the surfaces of $l = const.$ and the surfaces of $\Omega = const.$ coincide so one can introduce the function

$$F = (1 - \Omega l) \exp \int_{l_{in}}^{l} (1 - \Omega l)^{-1} \Omega \mathrm{d}l, \tag{2.62}$$

where $l_{in}$ denotes the value of $l$ on the inner edge of the torus. The time component of four-velocity $u^t = A$ is called the redshift factor and $u_t = U$ is the energy of the fluid element per unit inertial mass. From the normalization condition for four-velocity we get:

$$A = (-g_{tt} - 2\Omega g_{t\varphi} - g_{\varphi\varphi}\Omega^2)^{-\frac{1}{2}}, \tag{2.63}$$

$$U = (g_{\varphi\varphi} + 2l g_{t\varphi} + l^2 g_{tt})^{-\frac{1}{2}} ({g_{t\varphi}}^2 - g_{tt} g_{\varphi\varphi})^{\frac{1}{2}}, \tag{2.64}$$

$$AU = (1 - \Omega l)^{-1}. \tag{2.65}$$

For details see (A5a) and (A5b) in appendix. The solution of relativistic Euler equation (2.50)

$$\frac{p_{,\mu}}{p + \epsilon} = (\ln A)_{,\mu} - \frac{l\Omega_{,\mu}}{1 - \Omega l}, \tag{2.66}$$

where $\epsilon$ denotes the total energy density in the rest frame, can be rewritten in two equivalent forms:

$$W - W_{in} \equiv \ln(FA)_{in} - \ln(FA) = -\int_0^p \frac{\mathrm{d}p}{p + \epsilon}, \tag{2.67}$$

and

$$W - W_{in} = \ln U - \ln U_{in} - \int_{l_{in}}^{l} \frac{\Omega \mathrm{d}l}{1 - \Omega l} = -\int_0^p \frac{\mathrm{d}p}{p + \epsilon}, \tag{2.68}$$

where we have used (2.65) and (2.62). The quantity $W = W(p)$ is equal to the total potential in Newtonian limit (expressed in the units of $c^2$). Therefore $W = 0$ at infinity. In the isentropic case considered by Fishbone & Moncrief (1976) we get

$$\int_0^p \frac{\mathrm{d}p}{p + \epsilon} = \ln\left(\frac{h}{h_{in}}\right), \tag{2.69}$$

where $h = \frac{p+\epsilon}{n}$ is the specific enthalpy. In any case the isobaric (equipotential) surfaces are given by the equation $W = const.$ For a known background gravitational field and a given von Zeipel's relation it is easy to determine the explicit form of the equation $W(r, \theta) = const.$ from (2.61) and (2.68). Thus, the problem of constructing the model of torus is completely solved.

Now we are ready to give explicit solutions for tori with following properties:

$$l = const. \tag{2.70}$$

or

$$l_* \equiv \frac{l}{1 - \Omega l} = const. \tag{2.71}$$

The second relation was used by Fishbone & Moncrief (1976). In the case of $l = const.$ it is easy to see from equation (2.68) that

$$W = -\ln[A(1 - \Omega l)] = \ln U. \tag{2.72}$$

In the case $l_* = const.$ we get

$$W = -\ln A + l_* \Omega. \tag{2.73}$$

(For details see Abramowicz & Jaroszynski (1977)). So for the case of $l = const$ we have

$$W - W_{in} = \ln U - \ln U_{in} = -\int_0^P \frac{\mathrm{d}p}{p + \rho_0 + u}, \tag{2.74}$$

where $p$ means the pressure, $\rho_0$ is the rest mass density and $u$ is the density of internal energy.

## 2.3 Magnetized torus with the toroidal magnetic field

We now assume that the magnetic field is present in the torus. In this case the energy-momentum tensor can be written in this form:

$$T^{\mu\nu} = (w + b^2)u^\mu u^\nu + \left(p + \frac{1}{2}b^2\right) g^{\mu\nu} - b^\mu b^\nu, \tag{2.75}$$

where $w$ is the specific enthalpy ($w = \rho_0 + p + u$), $p$ is the pressure and $b^\mu$ is the projection of magnetic field vector defined in section 1.1. Our assumptions of the flow are same as in the previous chapter. We will restrict ourselves in the cases of pure azimuthal magnetic fields ( satisfying $b^r = b^\vartheta = 0$ ). The covariant equations of ideal relativistic MHD are energy-momentum tensor conservation, continuity equation and Maxwell's equations. In our case the only non-trivial result follows from energy-momentum tensor conservation $T^{\mu\nu}_{\ ;\nu} = 0$. Contracting this equation with projection

tensor $h^{\mu}{}_{\nu}$ defined in section 1.1 we obtain (see appendix in Komissarov (2006) for details)

$$(w+b^2)u_\nu u^\nu_{,i} + \left(p+\frac{b^2}{2}\right)_{,i} - b_\nu b^\nu_{,i} = 0, \tag{2.76}$$

where $i = r, \vartheta$. We can rewrite this equation in terms of the angular velocity $\Omega = \frac{u^\varphi}{u^t}$ and the angular momentum $l = -\frac{u_\varphi}{u_t}$. Then we get

$$(\ln|u_t|)_{,i} - \frac{\Omega}{1-l\Omega}l_{,i} + \frac{p_{,i}}{w} + \frac{(\mathcal{L}b^2)_{,i}}{2\mathcal{L}w} = 0, \tag{2.77}$$

where $\mathcal{L}(r,\vartheta) \equiv {g_{t\varphi}}^2 - g_{tt}g_{\varphi\varphi}$. When $b^2 \to 0$ then equation (2.77) reduces to equation (2.66). For a barotropic equation of state ($w = w(p)$) from equation (2.77) it follows that

$$\mathrm{d}\left(\ln|u_t| + \int_0^P \frac{\mathrm{d}p}{w}\right) - \frac{\Omega}{1-l\Omega}\mathrm{d}l + \frac{\mathrm{d}(\mathcal{L}b^2)}{2\mathcal{L}w} = 0 \tag{2.78}$$

In the non-magnetized torus case, this equation implies that $\Omega = \Omega(l)$ and so the surfaces of constant $\Omega$ and $l$ coincide. But there is no reason to be fulfilled this relation for magnetized tori case. However, if we still assume that $\Omega = \Omega(l)$ from some reason, then we can rewrite equation (2.78) as

$$\ln|u_t| + \int_0^P \frac{\mathrm{d}p}{w} - \int_0^l \frac{\Omega \mathrm{d}l}{1-\Omega l} + \int_0^{\tilde{p_m}} \frac{\mathrm{d}\tilde{p_m}}{\tilde{w}} = const., \tag{2.79}$$

where $\tilde{w} \equiv \mathcal{L}w$, $\tilde{p_m} \equiv \mathcal{L}p_m$ and $p_m = \frac{b^2}{2}$ is the magnetic pressure. On the surface of the torus and also on its inner edge there is

$$p = p_m = 0, u_t = u_{t_{in}}, l = l_{in}. \tag{2.80}$$

So we can find the constant of integration as

$$const. = \ln|u_{t_{in}}| - \int_0^{l_{in}} \frac{\Omega \mathrm{d}l}{1-\Omega l}. \tag{2.81}$$

Now we assume (as in the section 2.2) that $l$ is the constant through the torus. Then we can rewrite equation (2.79) into following form

$$W - W_{in} + \int_0^P \frac{\mathrm{d}p}{w} + \int_0^{\tilde{p_m}} \frac{\mathrm{d}\tilde{p_m}}{\tilde{w}} = 0. \tag{2.82}$$

In (A6) in appendix there is shown that for the non-zero components of $b^\mu$ the following expressions are valid:

$$b^\varphi = \pm\sqrt{\frac{2p_m}{\mathcal{A}}}$$

and

$$b^t = lb^\varphi, \tag{2.83}$$

where $\mathcal{A} \equiv g_{\varphi\varphi} + 2lg_{t\varphi} + l^2 g_{tt}$.

# 3. Results: axi-symmetric accretion of magnetized tori

## 3.1 The dependence of accretion rates on magnetic field

We will assume at first the non-magnetized Abramowicz et al. model of accretion torus ($l = const.$) with the polytropic equation of state:

$$p = \kappa \rho_0^{\gamma},$$
$$u = \frac{p}{\gamma - 1}. \tag{3.1}$$

For the special choice of $\gamma = \frac{4}{3}$ and $\kappa = 10^{-2}$ , which are physically relevant, we can solve the right hand side of equation (2.74) analytically and write the result as

$$\ln U - \ln U_{in} = -\ln\left(1 + \frac{p^{\frac{1}{4}}}{0.25 \cdot 10^{\frac{3}{2}}}\right). \tag{3.2}$$

In our scheme of constructing the torus, we need to express the thermodynamical variables as a function of the metric only. So we rewrite the last equation into following form:

$$p = \left(\frac{U_{in}}{U} - 1\right)^4 \cdot 25^4 \cdot 10^{-2}. \tag{3.3}$$

From equation (3.3) we can obtain the value of pressure at each point of the torus and via equations (3.1) the rest mass density and density of internal energy too.

If we want to assume a magnetic field in the torus we must solve equation (2.82), which is more complicated than equation (2.74). We could solve this equation numerically of course but it would be a next possible source of numerical noise. We impose the relation between the both integrals in equation (2.82) so, that

$$\int_0^P \frac{\mathrm{d}p}{w} = const. \cdot \int_0^{\tilde{P_m}} \frac{\mathrm{d}\tilde{p_m}}{\tilde{w}}. \tag{3.4}$$

The solution of the first integral is already known and so the equation (2.82) reduces to

$$\ln\left(\frac{U_{in}}{U}\right) = \left(1 + \frac{1}{const.}\right) \ln\left(1 + \frac{p^{\frac{1}{4}}}{0.25 \cdot 10^{\frac{3}{2}}}\right), \tag{3.5}$$

from which it follows that

$$p = \left[\left(\frac{U_{in}}{U}\right)^{\frac{const.}{1+const.}} - 1\right]^4 \cdot 25^4 \cdot 10^{-2}. \tag{3.6}$$

Since we need to know the magnetic pressure at each point of the torus, we must impose the dependence of $\tilde{p_m}$ on $\tilde{w}$. From equation (2.78) it is obvious that the last term is a total differential and so one can write

$$\tilde{p_m} = K_m \tilde{w}^\eta, \tag{3.7}$$

where $K_m$ and $\eta$ are constants. Now it is easy to see that

$$\int_0^{\tilde{P_m}} \frac{\mathrm{d}\tilde{p_m}}{\tilde{w}} = \frac{\eta}{\eta - 1} {K_m}^{\frac{1}{\eta}} {\tilde{p_m}}^{\frac{\eta-1}{\eta}}. \tag{3.8}$$

Since we have analytically evaluated both integrals, we can rewrite $\tilde{p_m}$ in terms of $p$. We get following expression:

$$\tilde{p_m} = \left[ \frac{1}{const.} \frac{\eta - 1}{\eta} {K_m}^{-\frac{1}{\eta}} \ln\left(1 + \frac{p^{\frac{1}{4}}}{25 \cdot 10^{\frac{1}{4}}}\right) \right]^{\frac{\eta}{\eta-1}}. \tag{3.9}$$

One can see that there are three free parameters: *const.*, $\eta$ and $K_m$. We must be very careful which values of these parameters we take. For some special choices of these parameters we can get too big gradients of magnetic field which causes a numerical noise. In our computation we adopted these values: *const.* $= 100$, $\eta = \frac{4}{3}$. Changing the value of $K_m$ we were getting different ratios of thermodynamical pressure to magnetic pressure $\beta$.

In Figure 3.1 there is shown an image produced by HARM. There is expressed $l = const.$ torus which ranges from $r_{in} = 5M_{B.H.}$ to $r_{out} = 10M_{B.H.}$ (hereafter we will use units in which the black hole mass $M_{B.H.}$ is equal to one and $c = G = 1$), where $r_{in}$ and $r_{out}$ denote the inner and outer edge of the torus. Different colors represents the rest mass density values which are normalized to the maximum value. The red color corresponds to the maximum and blue to the minimum. Especially for the torus in Figure 3.1 the maximum value of rest mass density is $100,000$ times bigger than the value on the surface of the torus. Since we adopted a Kerr spacetime and assume that the torus does not influence it, the total rest mass of tori that we studied here was about 2% of black hole rest mass $M_{B.H.}$. There is a special choice of coordinate system in these images, where on the x-axis there is $\ln r$ and on the y-axis there is a special function of $\vartheta$ so that vertical line on this picture corresponds to a contant $r$. The left-side corner of the picture corresponds to $r = 1.96M_{B.H.}$ and right-side corner corresponds to $r = 20M_{B.H.}$ (this is valid for all images of accretion torus in Schwarzschild spacetime).

In Figure 3.2 there is the same torus as in Figure 3.1 but in "usually used" Schwarzschild coordinates. On x-axis there is $r \cdot \sin\vartheta$ and on y-axis there is $r \cdot \cos\vartheta$. So we can see realistic shape of the torus.

Now we investigate the dependence of accretion rate on the magnetic field. At first there is a purely azimuthal flow in the torus in both non-magnetized and magnetized tori. We perturb this state by increasing the black hole mass. At first we focus on

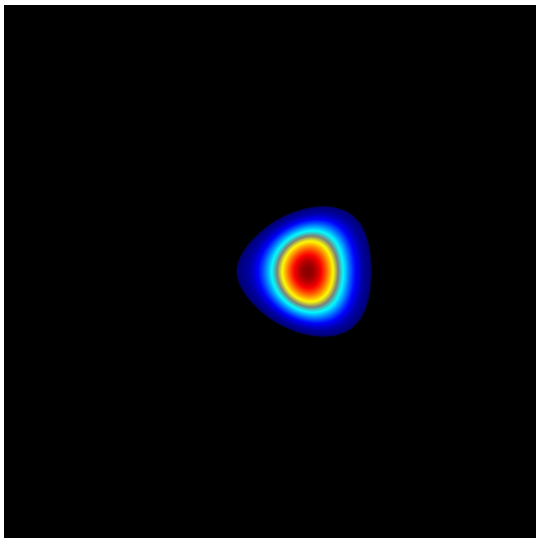

Figure 3.1: Demonstration of image produced by HARM.

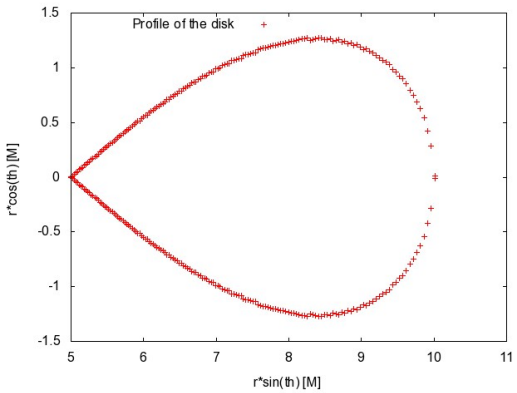


Figure 3.2: Profile of $l = const.$ torus in Schwarzschild coordinates.

the case of Schwarzschild spacetime and the torus with cusp ($r_{in} = 5.0$, $l = \frac{5\sqrt{5}}{3}$). The torus has cusp if on its inner edge the following relation is fulfilled:

$$l = l_K = \frac{r^2 - 2a\sqrt{r} + a^2}{r^{\frac{3}{2}} - 2\sqrt{r} + a}, \tag{3.10}$$

where $l_K$ denotes the Keplerian angular momentum. In the stationary situation there is no accretion as we can see from Figure 3.3 where is the non-magnetized torus and from Figure 3.4 where is magnetized torus with the ratio of pressure to magnetic pressure $\beta$ equal to $\beta = 31.009$. The orbital period at the inner edge of the torus ($r_{in}$) is approximately equal to 70.

Now we assume that the black hole increases its mass somehow from $1M_{B.H.}$ to $1.01M_{B.H.}$ so we have not the purely azimuthal flow and the torus will start to accrete on black hole as we can see in Figure 3.5 and Figure 3.6. In Table 3.1 there is

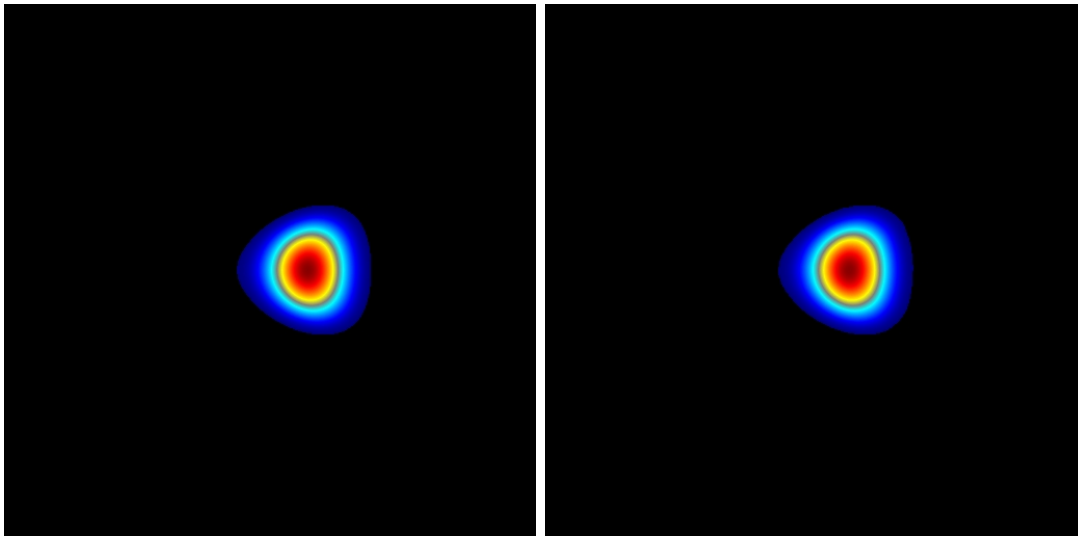

(a) t=0 (b) t=200

Figure 3.3: Non-magnetized torus, $a = 0$.

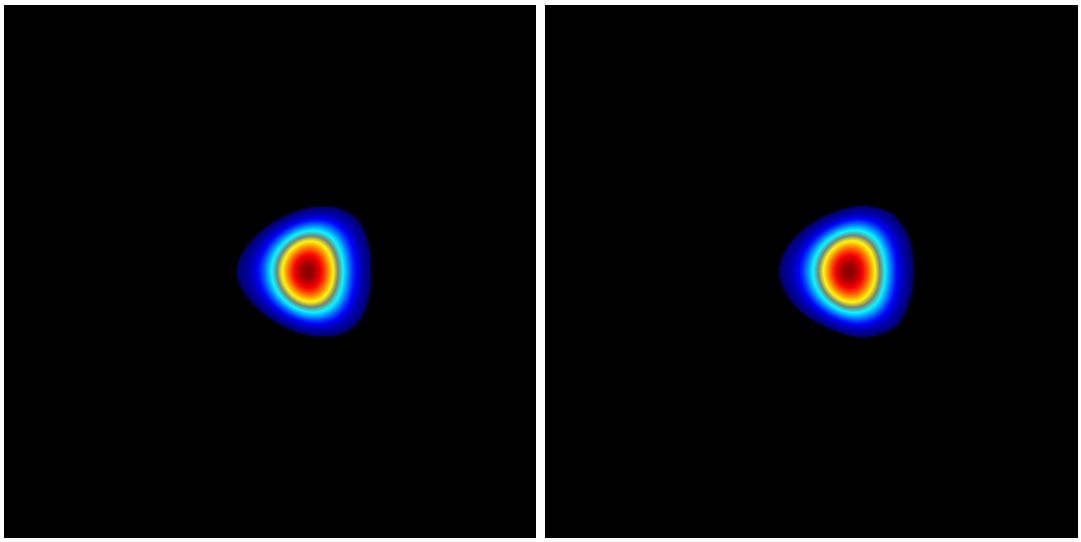

(a) t=0 (b) t=200

Figure 3.4: Magnetized torus, $a = 0$, $\beta = 31.009$.

expressed the dependence of accretion on the value of $\beta$ in this perturbed case. We express the accretion in terms of how much rest mass of the torus in $t = 0$ is accreted in $t = 200$. It means how much rest mass of the initial torus is closer to black hole than the inner edge of the initial torus ($5M_{B.H.}$).

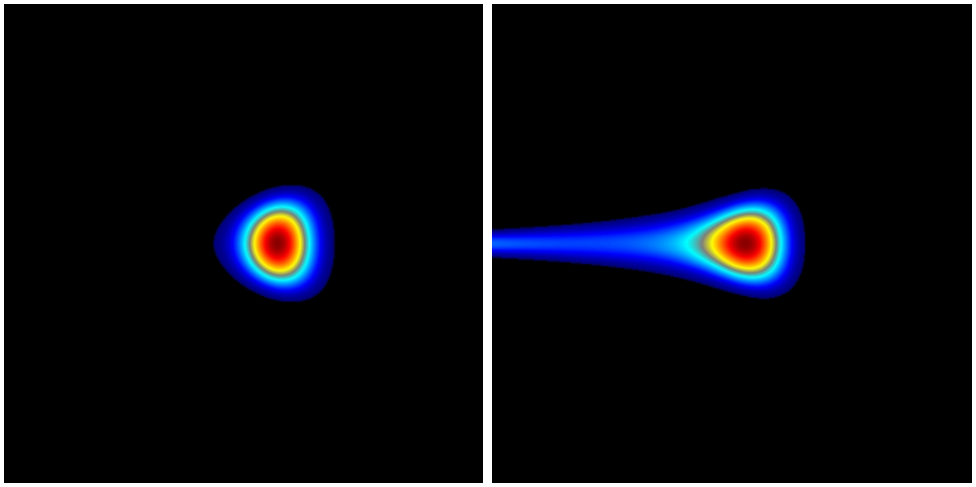

(a) t=0 (b) t=200

Figure 3.5: Non-magnetized torus, $a = 0$, perturbed version.

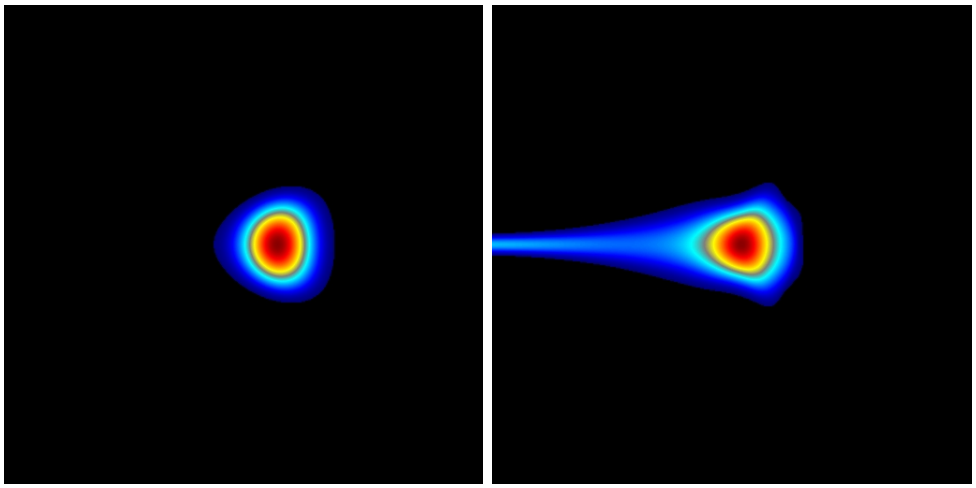

(a) t=0 (b) t=200

Figure 3.6: Perturbed version, $a = 0$, $\beta = 3.891$.

| $\beta$ | accreted mass [%] in $t = 120$ | accreted mass [%] in $t = 200$ |
|---|---|---|
| 3.891 | 7.84 | 19.55 |
| 13.133 | 6.37 | 17.63 |
| 31.129 | 5.96 | 17.05 |
| 105.060 | 5.74 | 16.73 |
| 486.391 | 5.66 | 16.62 |
| $\infty$ | 3.43 | 12.23 |

Table 3.1

Now we leave the Schwarzschild spacetime and step forward to Kerr spacetime

with $a = 0.1$. We employ the torus with the cusp again. The inner edge of the torus is on $r_{in} = 5.0$ the outer edge is $r_{out} = 7.7536$. The orbital period of inner edge of the torus is approximately 72. In the figures the left corner corresponds to $r = 1.955$ and the right corner corresponds to $r = 10$. In Figure 3.7 there is the torus in stationary state without magnetic field and in Figure 3.8 there is the torus in stationary state with $\beta = 23.192$. One can see that the profile of the torus in $t = 120$ is not as smooth as in $t = 0$, but there is still no accretion since the mass of the torus remains constant. The non-smooth profile of the torus in $t = 120$ is caused by numerical noise. For comparison with the torus in Schwarzschild case ($a = 0$), there are profiles of both these tori in Figure 3.9 in Schwarzschild coordinates .

We turn our attention on the perturbed case again. We assume that the black hole mass was increased from $1M_{B.H.}$ to $1.01M_{B.H.}$. In Figure 3.10 there is the perturbed case with zero magnetic field.

In Figure 3.11 there is the perturbed version of magnetized torus with $\beta = 23.297$. The dependence of accretion rate on the value of magnetic field is shown in Table 3.2, where is expressed the relative lost of mass in $t = 60$ and $t = 120$ (the orbital period of inner edge of the torus is approximately 72).

| $\beta$ | accreted mass [%] in $t = 60$ | accreted mass [%] in $t = 120$ |
|---|---|---|
| 2.912 | 2.32 | 33.24 |
| 23.297 | 1.83 | 31.50 |
| 78.626 | 1.78 | 31.25 |
| 186.374 | 1.78 | 31.19 |
| 364.011 | 1.77 | 31.18 |
| $\infty$ | 1.77 | 31.18 |

Table 3.2

If we compare the data from Tables 3.1 and 3.2 in $t = 120$ and realizing that the orbital periods does not differ very much ($T_{a=0} = 70.2$ and $T_{a=0.1} = 72.1$) we can see that the accretion for $a = 0.1$ case is more significant than in the case of $a = 0$. The main reason is probably the fact that the torus in $a = 0.1$ case is smaller and its maximal rest mass density is closer to black hole. So the bigger value of rest mass can pass through the torus and leave it. We can also see from Table 3.2 that for smaller times the relative differences of accreted mass between the cases of different $\beta$ are more significant than for bigger times. So it appears that the magnetic field plays more important role for earlier phases of accretion. It is surprising if we realize that the accretion causes the magnetic field not to be toroidal anymore and so the "chaotic" magnetic field should increase the corruption of initial equilibrium in the torus. One could expect that the magnetic field will be more chaotic in time and so the accretion will be faster. From these simulations it appears that even if the magnetic field strength is significant (it means that the magnetic pressure is comparable with the thermodynamical pressure) it does not play very important role in cases when the significant part of the accretion torus is accreted. But if

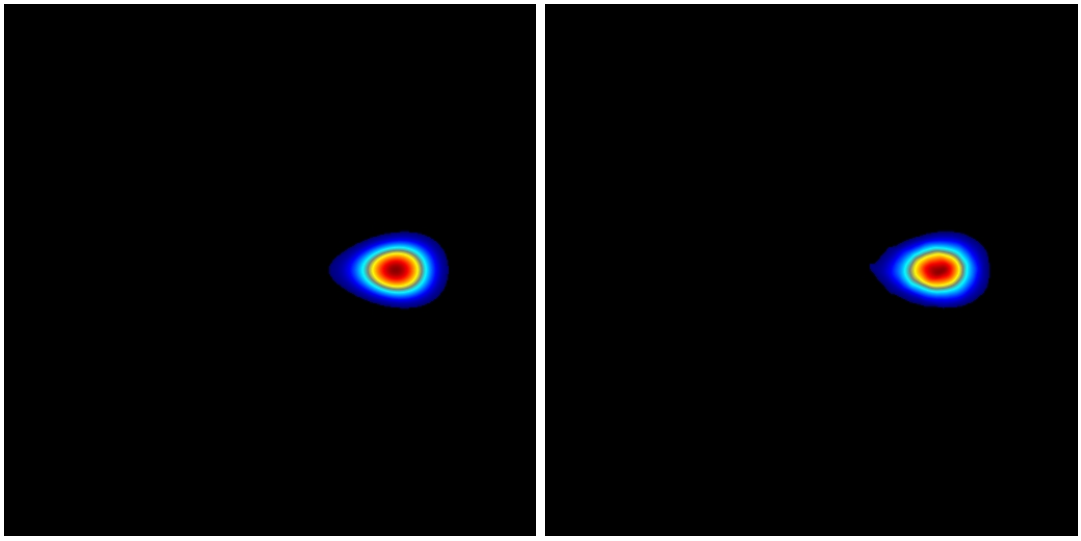

(a) t=0 (b) t=120

Figure 3.7: Non-magnetized torus, $a = 0.1$.

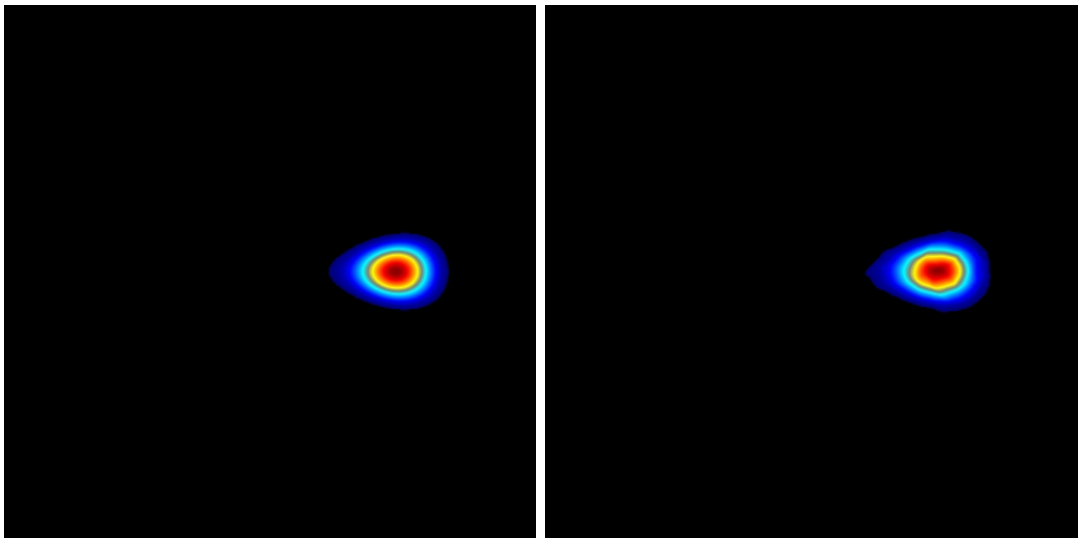

(a) t=0 (b) t=120

Figure 3.8: Magnetized torus, $a = 0.1$, $\beta = 23.192$.

the accretion is small (the addition of mass to black hole is small) the presence of magnetic field plays important role. From the observations of $SgrA^*$ we know that the magnetic field strength can reach the value around $40G$ (Eckart et al. 2008). When we take as the black hole mass the mass of $SgrA^*$ (approximately $4 \cdot 10^6 M_\odot$) the biggest values of magnetic field which we get (in the center of torus, where is the biggest thermodynamical pressure too) are several thousands of Gauss. These values corresponds to $\beta = 1$. It means that for $\beta \approx 100$ we could get the magnetic

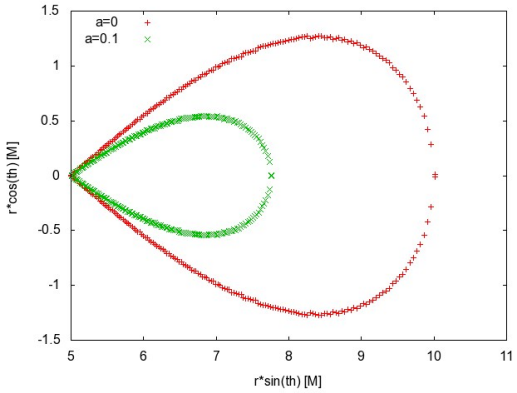


Figure 3.9: Tori of $l = const$ for $a = 0$ and $a = 0.1$.

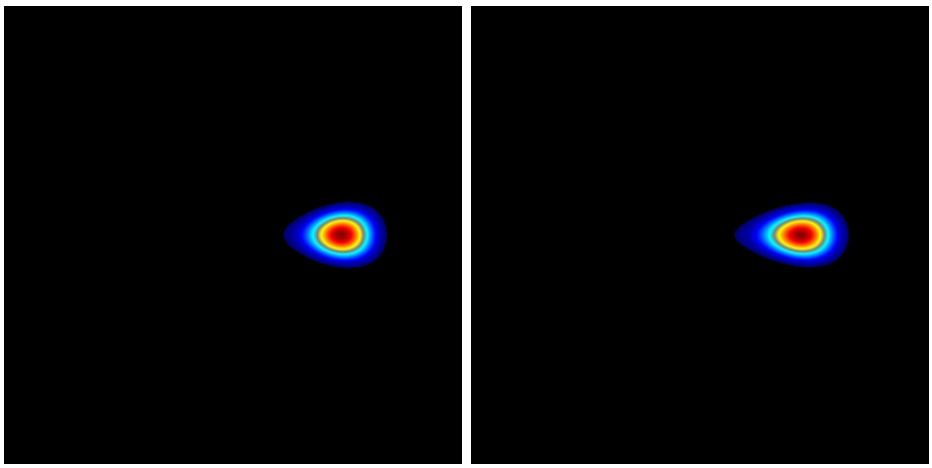

(a) t=0 (b) t=40

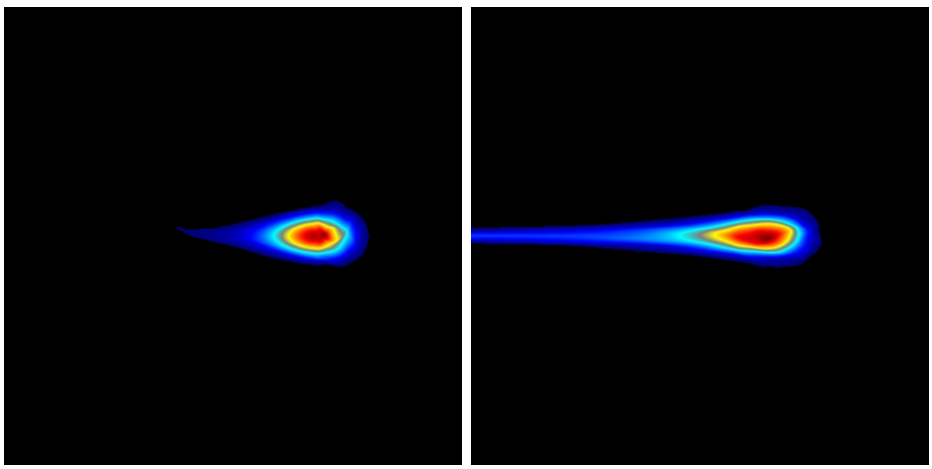

(c) t=80 (d) t=120

Figure 3.10: Perturbed version of non-magnetized torus, $a = 0.1$.

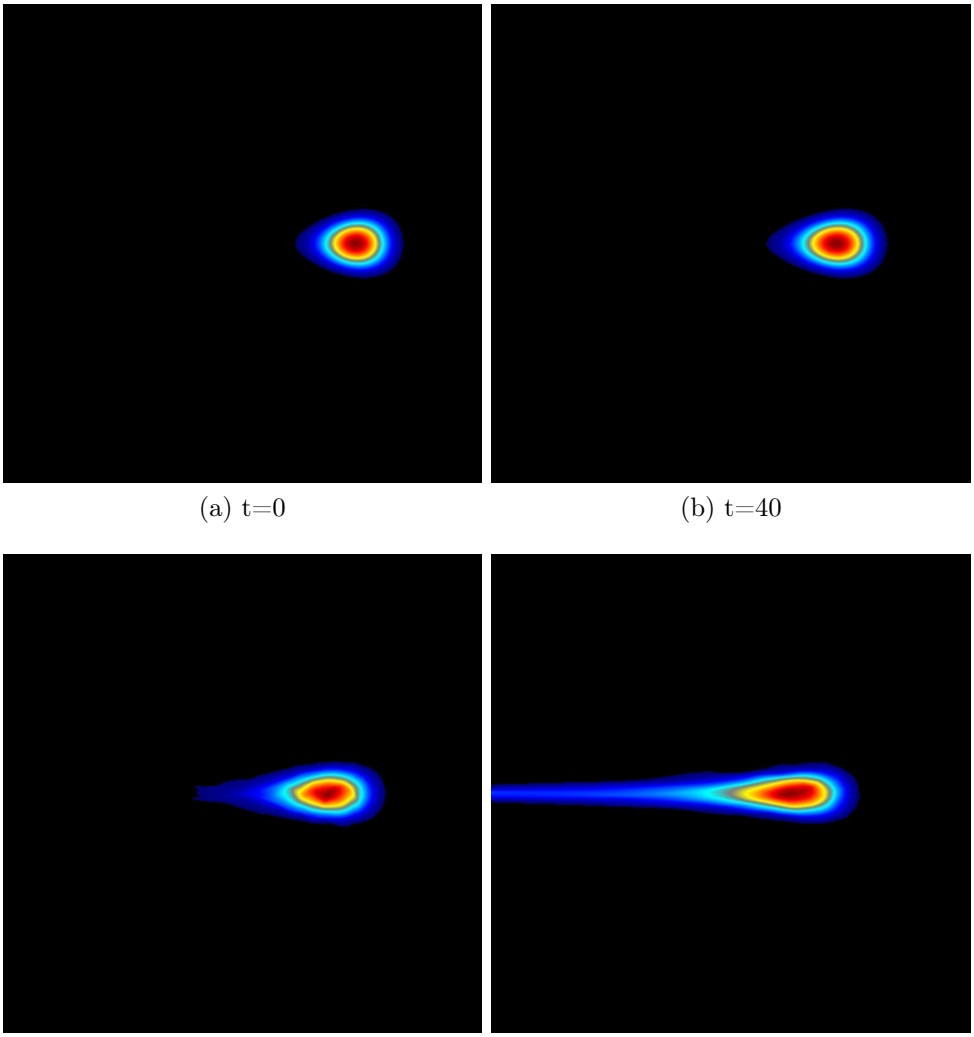

(a) t=0 (b) t=40

(c) t=80 (d) t=120

Figure 3.11: Perturbed version of magnetized torus, $a = 0.1$, $\beta = 23.297$.

field strength which would be comparable with observed magnetic field strength. On the other hand the maximal value of rest mass density (and so the value of maximal thermodynamical and magnetic pressure) depends on $r_{in}$ and $l$ strictly. For example for the torus of $r_{in} = 5.8$ and $l = 4.156$ which we consider in next section the maximal magnetic field strength (for $\beta = 1$) would be several Gauss roughly.

## 3.2 Comparison of $l$=*const.* and $l_*$=*const.* tori

If we want to compare the Fishbone-Moncrief torus and $l = const.$ torus we have to mention that, thanks to a different dependence of angular momentum in these two cases, for a given $r_{in}$, $l$ and $l_*$ according to equation (2.71) these tori have a different range and in some cases both of them do not exist. It is a straight consequence of equation (2.31) from which one can see that the value of angular momentum $l$ influence the increasing or decreasing of $\ln h$ from the inner boundary. From (2.71) we can also see that if $l$ is constant through the torus, $l_*$ is decreasing with the radial distance $r$ or, if $l_*$ is constant, the corresponding $l$ is increasing.

In Figure 3.12 there is $l = const.$ torus with $r_{in} = 5.8$, $l = 4.156$ and in Figure 3.13 there is a Fishbone-Moncrief torus with $r_{in} = 5.8$, $l_* = 5.0$. We did this choice to have both tori with the same $r_{in}$ and $r_{out}$ ($r_{out} = 149.98$ ). The orbital periods of these two types of accretion torus are: $T_{orbit} = 77.6$ for $l = const.$ torus and $T_{orbit} = 87.6$ for Fishbone-Moncrief torus. The left-side corner of following images corresponds to $r = 1.96$ and the right-side corner corresponds to $r = 200$.

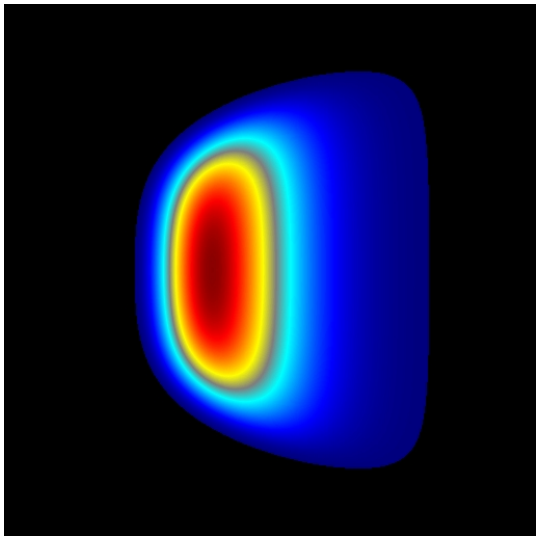

Figure 3.12: Torus of $l = const.$.

Another significant difference between $l = const.$ torus and Fishbone-Moncrief torus is the presence of cusp because Fishbone-Moncrief tori have no cusps (Fishbone & Moncrief 1976). It is a consequence of the fact that $\ln h$ in (2.31) depends on $\sin^2\vartheta$ in a sufficiently regular way as we discussed in section 2.1. We want to compare accretion rates of these tori when the mass of black hole is enhanced from $1M_{B.H.}$ to $1.1M_{B.H}$. In Figure 3.14 there is Fishbone-Moncrief torus and in Figure 3.15 there is $l = const.$ torus.

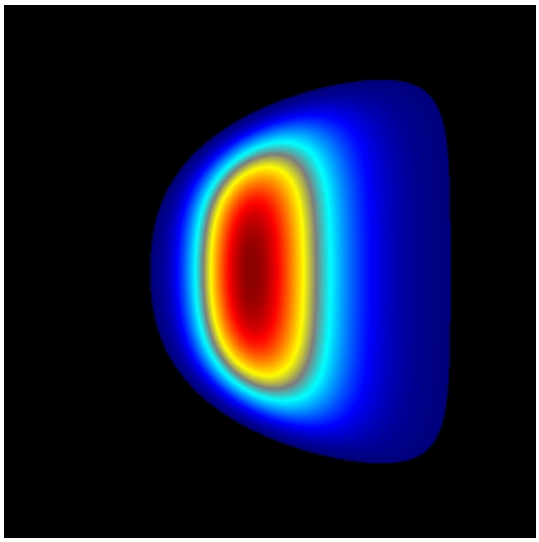

Figure 3.13: Fishbone-Moncrief torus.

| $t$ | accreted mass [%] for $l = const.$ torus | accreted mass [%] for F.-M. torus |
|---|---|---|
| 50 | 0.0004 | 0 |
| 100 | 0.426 | 0.063 |
| 150 | 0.911 | 0.160 |
| 200 | 1.311 | 0.251 |
| 300 | 1.912 | 0.390 |
| 400 | 2.413 | 0.488 |

Table 3.3

We can see that the Fishbone-Moncrief torus is more resistant against the perturbation caused by increasing the black hole mass. It is not surprising since we know that in the Fishbone-Moncrief torus with $l_* = const.$ the angular momentum density $l$ increase its value from the inner boundary. At this place it is important to emphasize that we have compared two special cases of accretion torus and so we can not give some general conclusions which would determine some relations between the Fishbone-Moncrief and $l = const.$ tori. We compared two tori with same $r_{in}$ and $r_{out}$ which had different angular momentum density dependence and so different distribution of rest mass density and pressure. In Table 3.3 there is expressed the time dependence of accreted rest mass. In Figures 3.15 and 3.14 we can nicely see the different properties of accretion process. In the Fishbone-Moncrief case the accretion flow decreases itself from $t = 150$ to $t = 400$ in contrast to $l = const.$ case.

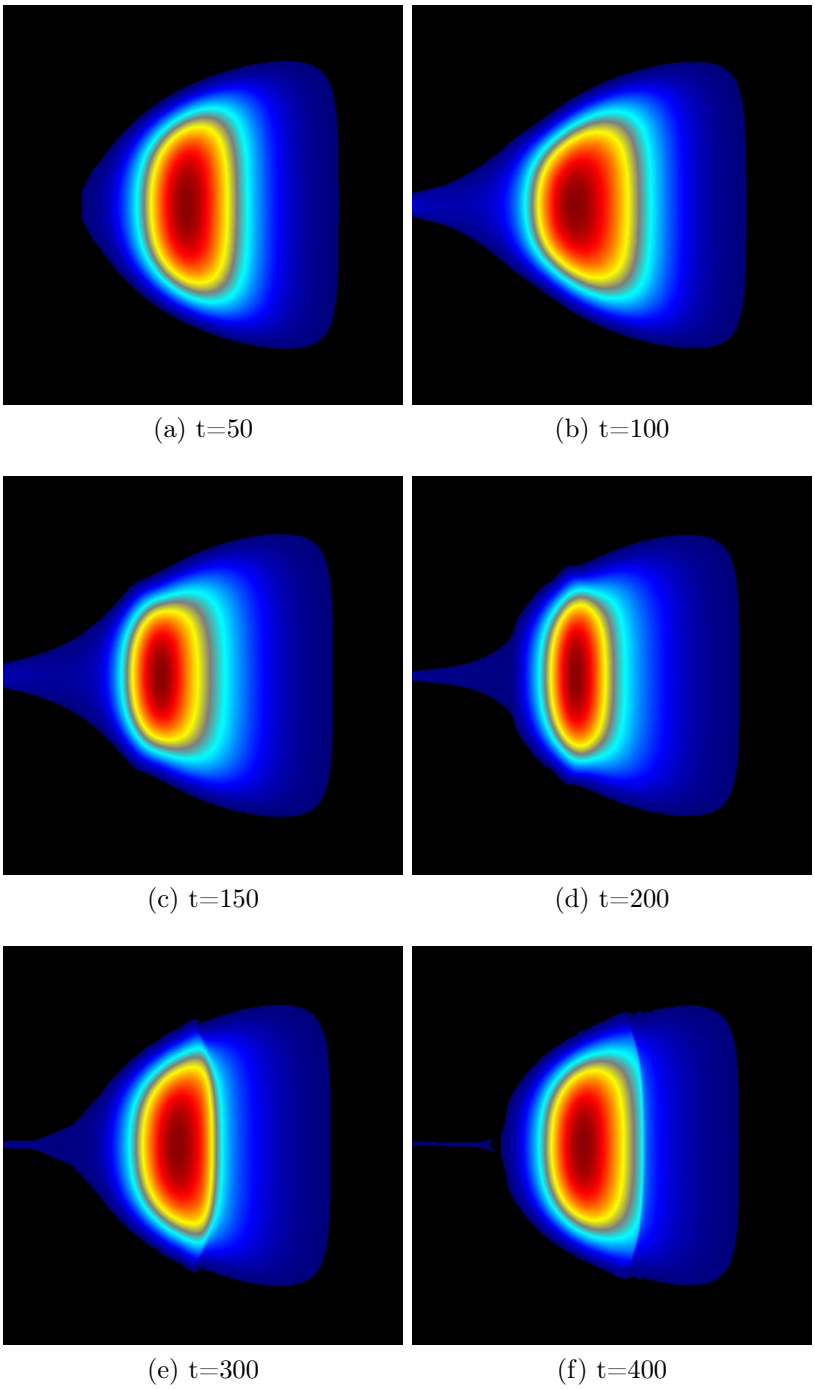

(a) t=50 (b) t=100

(c) t=150 (d) t=200

(e) t=300 (f) t=400

Figure 3.14: Perturbed version of Fishbone-Moncrief torus.

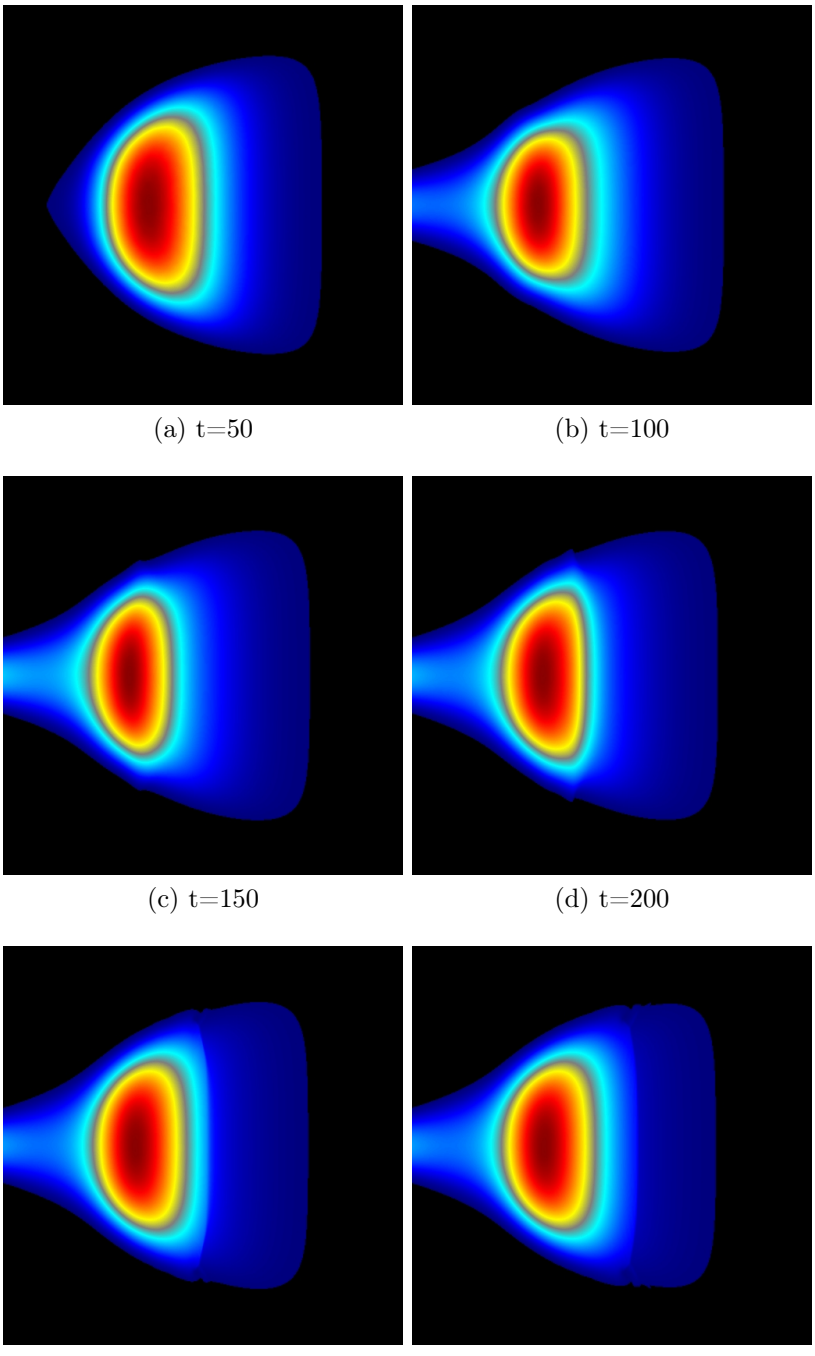

(a) t=50 (b) t=100

(c) t=150 (d) t=200

(e) t=300 (f) t=400

Figure 3.15: Perturbed version of $l = const.$ torus.

# Conclusion

In this diploma thesis we summarized two models of accretion torus: the torus with constant density of angular momentum (Abramowicz & Jaroszynski 1977) and Fishbone-Moncrief torus (Fishbone & Moncrief 1976). The properties of these tori were treated by solving General Relativistic MHD whose theoretical and numerical scheme was described in Chapter 1. We studied behavior of these tori when the mass of black hole, which the torus is orbiting, is increased suddenly and the purely azimuthal flow of the torus is corrupted and the accretion occurs. From the simulation it is obvious that for our special choice of parameters the Fishbone-Moncrief torus is influenced less than $l = const.$ torus by this perturbation.

We studied the influence of the value of toroidal magnetic field on accretion rate in the perturbed case. At first we focused on Schwarzschild spacetime and then on Kerr spacetime with $a = 0.1$. The tori were in equilibrium initially, but with different values of magnetic pressure. It occurred that the magnetic field plays important role at the beginning of accretion, but for higher times $t$ the relative differences in accreted mass between tori with different value of magnetic pressure are smaller than for earlier times $t$.

Models of magnetized accretion flows are relevant for the discussion of processes taking place in Galactic center. Naturally, while the conditions in the Galactic center are generally very complex, with turbulent sub-equipartition magnetic fields permeating a highly diluted medium, we have considered an idealized case. The main simplification adopted in our work is the assumption about axial symmetry of the flow, although we took time-dependence of the flow and the magnetic field into account and we evolved both toroidal and spoloidal components of the flow velocity. Hence, going to full three-dimensional motion is one possible direction of generalizing our approach, which many people consider as necessary to capture correctly the effects of magneto-rotational instability and to reproduce astrophysically realistic situations. Further, one should include also the role of radiation in the computations by coupling GRMHD equations to radiation transfer equations. These are of course much more complicated and computationally expensive systems, likely necessary to explain local enhancement of the field strength that have been reported in Galactic center flaresm reaching up to tens Gauss, i.e. greatly above the mean level.

One may, however, proceed further also with the restricted axisymmetric models. For example, we first intend to continue in our axisymmetric study of magnetized tori especially to focus on investigating the runaway instability for magnetized tori.

# Bibliography


Abramowicz, M. A., & Jaroszynski, M. 1977, General Relativity and Gravitation 1977, 64

Abramowicz, M. A. 1971, Acta Astronomica, 21, 81

Bardeen, J. M., Press, W. H., & Teukolsky, S. A. 1972, ApJ, 178, 347

Begelman, M. C., Blandford, R. D., & Rees, M. J. 1984, Reviews of Modern Physics, 56, 255

Eckart, A., et al. 2008, A&A, 479, 625

Fishbone, L. G., & Moncrief, V. 1976, ApJ, 207, 962

Gammie, C. F., McKinney, J. C., & Tóth, G. 2003, ApJ, 589, 444

Harten, A., Lax, P.D., & van Leer, B. 1983, SIAM Rev., 25, 35

Komissarov, S. S. 2006, Mon.Not.R.Astron.Soc., 368, 993

Kormendy, J., & Richstone, D. 1995, Annu. Rev. Astron. Astrophys., 33, 581

Lax, P. D., Wendroff, B. 1960, Commun. Pure Appl. Math. Vol. 13,No.140, 848

LeVeque, R.J. 1997, Computational Methods for Astrophysical Fluid Flow, Saas-Fee Advanced Course 27 Lecture Notes, New York:Springer,p.1

Noble, S. C., Gammie, C. F., McKinney, J. C., & Del Zanna, L. 2006, ApJ, 641, 626

Punsly, B. 2008, Black Hole Gravitohydromagnetics (Berlin: Springer)

Tóth, G. 1998, Computational Magnetohydrodynamics, Notes for an introductory level course

# Appendix

## A1 equation (1.26)

$$
\begin{aligned}
T^{\mu\nu}_{elmag} &= \frac{n^\mu \tilde{B}^\lambda n^\nu \tilde{B}_\lambda \cdot (-n_\mu u^\mu)(-n_\nu u^\nu)}{\gamma \cdot \gamma} \\
&\quad - \frac{1}{4} g^{\mu\nu} \frac{(n^\lambda \tilde{B}^\delta n_\lambda \tilde{B}_\delta + n^\delta \tilde{B}^\lambda n_\delta \tilde{B}_\lambda) \cdot (-n_\lambda u^\lambda)(-n_\lambda u^\lambda)}{\gamma \cdot \gamma} \\
&= \frac{\tilde{B}^\lambda \tilde{B}_\lambda u^\mu u^\nu}{\gamma \cdot \gamma} + \frac{1}{4} g^{\mu\nu} \frac{2 \cdot \tilde{B}^\delta \tilde{B}_\delta u^\lambda u_\lambda}{\gamma \cdot \gamma} \\
&= h^\lambda{}_\mu b^\mu h^\sigma{}_\mu b^\mu g_{\sigma\lambda} u^\mu u^\nu + \frac{1}{2} g^{\mu\nu} h^\delta_\mu b^\mu h^\sigma{}_\mu b^\mu g_{\sigma\delta} u^\lambda u_\lambda \\
&= g^\lambda_\mu b^\mu g^\sigma_\mu b^\mu g_{\sigma\lambda} u^\mu u^\nu + \frac{1}{2} g^{\mu\nu} g^\delta_\mu b^\mu g^\sigma_\mu b^\mu g_{\sigma\delta} u^\lambda u_\lambda \\
&= b^2 u^\mu u^\nu - \frac{1}{2} g^{\mu\nu} b^2 \\
&= b^2 u^\mu u^\nu + \frac{1}{2} g^{\mu\nu} b^2 - b^\mu b^\nu
\end{aligned}
\tag{A1}
$$

where we used $b^\mu u_\mu = 0$, $\tilde{B}^\nu = \frac{1}{3}\gamma h^\nu{}_\mu b^\mu$, and $g^{\mu\nu} b^2 = g^{\mu\nu} b^\mu b_\mu = b^\mu b_\nu$.

## A2 equation (1.45)

$$
\begin{aligned}
\tilde{B}^\mu Q_\mu &= \gamma(w + b^2) u_\mu \tilde{B}^\mu + (n_\nu b^\nu) \frac{1}{\gamma} h_\mu{}^\nu \tilde{B}_\nu \tilde{B}^\mu \\
&= \gamma(w + b^2) u_\mu \tilde{B}^\mu + (n_\nu b^\nu) \frac{1}{\gamma} (\tilde{B}^\mu \tilde{B}_\mu + u^\mu \tilde{B}_\mu u^\nu \tilde{B}_\nu) \\
&= \gamma(w + b^2) u_\mu \tilde{B}^\mu + \frac{1}{\gamma^2} n_\nu (\tilde{B}^\nu + u^\nu u_\mu \tilde{B}^\mu)(\tilde{B}^2 + (u_\mu \tilde{B}^\mu)^2) \\
&= \frac{W}{\gamma} (u_\mu \tilde{B}^\mu)
\end{aligned}
\tag{A2}
$$

A3 equation (1.46)

$$
\begin{aligned}
Q_\mu n^\mu &= -\gamma^2(w+b^2) + \left(p+\frac{b^2}{2}\right) + (n_\nu b^\nu)^2 \\
&= -\gamma^2\left(w + \frac{1}{\gamma^2}\left[\tilde{B}^2 + (\tilde{B}^\mu u_\mu)^2\right]\right) + \left(p + \frac{1}{2\gamma^2}\left[\tilde{B}^2 + (\tilde{B}^\mu u_\mu)^2\right]\right) + (u_\mu \tilde{B}^\mu)^2 \\
&= -W - \tilde{B}^2 - (\tilde{B}^\mu u_\mu)^2 + p + \frac{\tilde{B}^2 + (\tilde{B}^\mu u_\mu)^2}{2\gamma^2} + (u_\mu \tilde{B}^\mu)^2 \\
&= -\frac{\tilde{B}^2}{2}(1+v^2) + \frac{(\tilde{B}^\mu Q_\mu)^2}{2W^2} - W + p
\end{aligned}
\tag{A3}
$$

A4 equation (1.49)

$$
\begin{aligned}
Q_\mu Q^\mu &= -\gamma^2(w+b^2)^2 - \left(p+\frac{b^2}{2}\right)^2 + (n_\nu b^\nu)^2 b^2 - 2\gamma(w+b^2)\left(p+\frac{b^2}{2}\right) u_\mu n^\mu \\
&\quad + 2\gamma(w+b^2)(n_\nu b^\nu) u_\mu b^\mu - 2\left(p+\frac{b^2}{2}\right)(n_\nu b^\nu) n_\mu b^\mu \\
&= -\gamma^2\left(w + \frac{1}{\gamma^2}\left[\tilde{B}^2 + (\tilde{B}^\mu u_\mu)^2\right]\right)^2 + 2\gamma^2\left(w + \frac{1}{\gamma^2}\left[\tilde{B}^2 + (\tilde{B}^\mu u_\mu)^2\right]\right) \cdot \\
&\quad \cdot \left(p + \frac{1}{2\gamma^2}\left[\tilde{B}^2 + (\tilde{B}^\mu u_\mu)^2\right]\right) - \left(p + \frac{1}{2\gamma^2}\left[\tilde{B}^2 + (\tilde{B}^\mu u_\mu)^2\right]\right)^2 \\
&\quad - 2p \cdot (u_\mu \tilde{B}^\mu)^2 \\
&= -\left(\frac{W}{\gamma} + \frac{1}{\gamma}\left[\tilde{B}^2 + \frac{(\tilde{B}^\mu Q_\mu)^2\gamma^2}{W^2}\right]\right)^2 + \left(2W + 2\left[\tilde{B}^2 + \frac{(\tilde{B}^\mu Q_\mu)^2\gamma^2}{W^2}\right]\right) \cdot \\
&\quad \cdot \left(p + \frac{1}{2\gamma^2}\left[\tilde{B}^2 + \frac{(\tilde{B}^\mu Q_\mu)^2\gamma^2}{W^2}\right]\right) - \left(p + \frac{1}{2\gamma^2}\left[\tilde{B}^2 + \frac{(\tilde{B}^\mu Q_\mu)^2\gamma^2}{W^2}\right]\right)^2 \\
&\quad - 2p\frac{(\tilde{B}^\mu Q_\mu)^2\gamma^2}{W^2} \\
&= -W^2(1-v^2) + 2Wp - p^2 + \tilde{B}^2\left(-\frac{W}{\gamma^2} + p(1+v^2) - \frac{(\tilde{B}^\mu Q_\mu)^2}{2W^2\gamma^2}\right) \\
&\quad + \frac{(\tilde{B}^\mu Q_\mu)^2\gamma^2}{W^2}\left(-\frac{W}{\gamma^2} + p(v^2-1)\right) - \frac{1}{4\gamma^4}\left(\tilde{B}^4 + \frac{(\tilde{B}^\mu Q_\mu)^4\gamma^4}{W^4}\right).
\end{aligned}
\tag{A4}
$$

## A5 equations (2.63) and (2.64)

From the normalization condition for four-velocity

$$u_\mu u^\mu = -1$$

and realizing that

$$u^\mu = (u^t, 0, 0, u^\varphi)$$

and

$$u^\varphi = u^t \Omega$$

we get

$$A^2(g_{tt} + 2\Omega g_{t\varphi} + g_{\varphi\varphi}\Omega^2) = -1,$$

from which follows:

$$A = \frac{1}{\sqrt{-(g_{tt} + 2\Omega g_{t\varphi} + g_{\varphi\varphi}\Omega^2)}}. \tag{A5a}$$

For $u_\varphi$ we can write:

$$u_\varphi = g_{t\varphi} A + g_{\varphi\varphi} A\Omega$$

and using the normalization condition we obtain

$$u_t A = -1 - (g_{t\varphi} A^2 \Omega + g_{\varphi\varphi} A^2 \Omega^2).$$

From the last equation we get

$$u_t (\equiv U) = \frac{-1 - g_{t\varphi} A^2 \Omega - g_{\varphi\varphi} A^2 \Omega^2}{A}.$$

Now we will use equation (A5a) to rewritte $U$ into form:

$$\begin{aligned} U &= \sqrt{-(g_{tt} + 2\Omega g_{t\varphi} + g_{\varphi\varphi}\Omega^2)} \cdot \frac{-g_{tt} - 2\Omega g_{t\varphi} - g_{\varphi\varphi}\Omega^2 + g_{t\varphi}\Omega + g_{\varphi\varphi}\Omega^2}{g_{tt} + 2\Omega g_{t\varphi} + g_{\varphi\varphi}\Omega^2} \\ &= \frac{-g_{tt} - g_{t\varphi}\Omega}{\sqrt{-(g_{tt} + 2\Omega g_{t\varphi} + g_{\varphi\varphi}\Omega^2)}}. \end{aligned}$$

We employ an expression for angular velocity $\Omega = -\frac{g_{t\varphi} + l g_{tt}}{g_{\varphi\varphi} + l g_{t\varphi}}$ , insert it into the last equation and after a simple algebraic manipulation we finally get:

$$U = \frac{\sqrt{{g_{t\varphi}}^2 - g_{tt} g_{\varphi\varphi}}}{\sqrt{g_{\varphi\varphi} + 2l g_{t\varphi} + l^2 g_{tt}}}. \tag{A5b}$$

## A6 equation (2.83)

From the normalization condition for four-velocity and assuming the symmetries for our problem it follows that

$$(u^t)^2 = -(g_{tt} + 2g_{t\varphi}\Omega + g_{\varphi\varphi}\Omega^2)^{-1}$$

and

$$u^t u_t = -\frac{1}{1 - l\Omega}.$$

From the last two equations and expression for $\Omega$ we get

$$(u_t)^2 = \frac{\mathcal{L}}{\mathcal{A}},$$

where $\mathcal{L}$ and $\mathcal{A}$ are defined in section 2.3. From the property of $b^\mu$ that $u_\mu b^\mu = 0$ and assuming that $u^r = u^\vartheta = b^r = b^\vartheta = 0$ we have

$$u^t b_t + u^\varphi b_\varphi = 0 \Rightarrow u^t b_t + u^t \Omega b_\varphi = 0 \Rightarrow b_t = -\Omega b_\varphi$$

and

$$b^t = l b^\varphi.$$

Now one can write

$$b^2 = b^\varphi b_\varphi (1 - \Omega l)$$

and

$$b^2 = (b^\varphi)^2 \mathcal{A}.$$

Finally we get

$$b^\varphi = \pm\sqrt{\frac{2p_m}{\mathcal{A}}} \tag{A6}$$